44 P.

1N-11103

C/S E7923857

FINAL REPORT

Title: Theoretical Study on The Effect of the Design of Small (milli-newton) Thruster Jets on Molecular Contamination for the Space Station.

Principle Investigator: Ben R. Riley
Department of Physics
University of Evansville
Evansville, IN 47722
(812)-479-2696

Date of Grant: November 15, 1985 to June 30, 1986

Grantee Institution: University of Evansville
1800 Lincoln Avenue
Evansville, IN 47722

Grant Number: NAG 3-674

PART 1

PRELIMINARY INFORMATION REPORT

SPACE STATION SYSTEM DIRECTORATE

LEWIS RESEARCH CENTER

Title: Molecular Column Densities Resulting from a Point Source Model

Author (s): Ben R. Riley

Present Address: Physics Department
University of Evansville
1800 Lincoln Avenue
Evansville, IN 47722

Division: Advanced Programs and Planning Office

Date: May 22, 1986

Distribution:
T. Labus
D. Schultz
D. Hoffman
G. Barna
P. Penko
J. Serafini
R. Tacina

INTRODUCTION

The self-induced on-orbit molecular contamination around the Space Station (SS) is of interest to anyone (user) anticipating doing experiments on or in the vicinity of the SS. Aerospace engineers need to design a SS propulsion system that keeps the SS in a stable orbit and at the same time does not allow the propellant gases to interfere with the experiments of the user. Another engineering consideration that has to be addressed in the SS design is a mechanism for venting waste gases.

One scenario that might accomplish the above requirements is to use an electrothermal propulsion system, resistojet, that will thrust continuously in the hundreds of milli-newton range which will provide a constant altitude for the SS with a low g environment. As a first attempt to understand the contamination from such a propulsion system, a point source model was developed in the summer of 1985 by Riley [1] at NASA - Lewis Research Center. This paper gives the numerical results of the point source model. Number column densities for CO_2 are presented in Table 1 as a function of direction of observation (line of sight), temperature of the exit gas, and mean exit velocity. One set of number column densities for N_2 is shown in Table 1 to contrast the effect of molecular weight. All the results are for a constant exhaust rate of 5,000 kg/year.

THE MODEL

Propellant gases from the jet nozzle are assumed to come from the jet exit plane with a mean macroscopic velocity $\vec{u}$ relative to the nozzle. The gases are assumed to be exhausted into a vacuum. Thus, there are no collisions with ambient molecules. At a distance of a few nozzle exit diameters from the nozzle, the gases will appear to come from a point.

The mathematical model developed (<u>using kinetic theory of gases</u>) allows one to calculate at any position and time the number density around a <u>point source</u> that has a Maxwellian velocity distribution.

Using the Boltzmann Equation one can write (see appendix A for nomenclature).

$$\frac{\partial f}{\partial t} + \vec{v} \cdot \nabla_r f = \delta(\vec{r})\, \varphi(t)\, \Phi(\vec{v}) \tag{1}$$

where

$$\Phi(\vec{v}) = \left(\frac{m}{2\pi k T}\right)^{3/2} e^{-\frac{m}{2kT}\left(\vec{v}-\vec{u}\right)^2} \tag{2}$$

and

$$n(\vec{r},t) = \iiint f(\vec{r},\vec{v},t)\, d^3 v \tag{3}$$

The assumptions in writing down equation (1) above are: (a) no external forces are exerted on the molecules, (b) the self-interaction terms are neglected, and (c) the source expands into a vacuum.

Using a constant flux source $Q(t)=Q_0$ and the Fourier-Laplace integral transform method, the result for the number density is

$$n(\vec{r},t) = \frac{Q_0}{2\pi r^2}\left(\frac{m}{2\pi kT}\right)^{1/2} e^{-\frac{m u^2}{2kT}\sin^2\theta}\left[e^{-\frac{m u^2}{2kT}\left(\frac{r}{ut}-\cos\theta\right)^2} + u\cos\theta\sqrt{\frac{m}{2kT}}\sqrt{\pi}\;\mathrm{erfc}\left(\frac{u}{\sqrt{2kT/m}}\left(\frac{r}{ut}-\cos\theta\right)\right)\right] \tag{4}$$

where $\cos\theta$ is defined by $\vec{r}\cdot\vec{u}$

where $\vec{r}$ is the location of the point that the number density n is to be calculated and $\vec{u}$ is the mean exit velocity. Both quantities are relative to the point source nozzle.

CALCULATIONS

In order to make the number density calculations as a function of θ, defined above, the erfc function in equation (4) was approximated (2) by

$$\mathrm{erfc}(x) = 1-\frac{2}{\sqrt{\pi}}\left(x - \frac{x^3}{3} + \frac{x^5}{10} - \frac{x^7}{42} + \frac{x^9}{216} - \frac{x^{11}}{1320} + \frac{x^{13}}{9360} - \frac{x^{15}}{75600} + \frac{x^{17}}{685440}\right) \tag{5}$$

for small values of the erfc argument, and by

$$\mathrm{erfc}(x) = \left(\frac{e^{-x^2}}{x\sqrt{\pi}}\right)\left(1 - \frac{1}{2x^2} + \frac{3}{(2x^2)^2} - \frac{15}{(2x^2)^3} + \frac{105}{(2x^2)^4} - \frac{945}{(2x^2)^5}\right) \tag{6}$$

for large values of the erfc argument. The transfer from equation 5 to equation 6 was made when x was greater than 1.68.

The point of observation was assumed to be 50 meters directly above the point source (see figure 1). Once one knows $n(\vec{r},t)$, the number density, it is a simple matter to calculate the number column density (NCD) by integrating numerically along a particular line of sight (LOS).

The number column densities as a function of the LOS were calculated for different temperatures at the exit plan (temperature of the gas at the point source) and different magnitudes of the mean exit velocity $\vec{u}$. The calculations were performed for the steady state situation for continuous firing. Therefore, the r/ut terms in equation (4) were assumed to be zero.

The number of CO_2 molecules per second, Q_o, exiting from the nozzle was assumed to be 2.2×10^{21}. For N_2 $Q_o=3.5\times10^{21}$. These values were obtained by assuming Q_o = 5,000 kg/year.

RESULTS

Table 1 gives the results for the NCD calculations as would be seen by an observer located 50 meters above the point source as indicated in fig. 1. The observation angle, ϕ, is defined in fig. 1 to be the angle between the line joining the observation point and the source and the line of sight. (For example, an angle of 270° for ϕ would mean a line of sight in the direction parallel to $\vec{u}$.)

The results of the NCD calculations are given in table 1 as a function of the temperature of the source, the mean exit velocity, and the line of sight.

All calculations were done in the plane containing a line connecting the source and observation point and the mean exit velocity vector.

Figures 2, 3, 5, 5, 6, and 7 respectively are graphical representations of the NCD's as a function of observation angle for the data presented as Case 1, 2, 3, 4, 5, and 6 respectively in Table 1. The exit temperatures are the same for figures 2 and 3 with the mean exit velocity being 4,000m/sec. and 1,000m/sec. respectively. Upon comparing the NCD's as a function of LOS in figures 2 and 3, one observes that higher column densities are prevalent at larger values of the angle between the LOS and the mean exit velocity vector which is at 270 ^{O} in figures 2 and 3. This implies that high mean exit velocities are necessary to increase the acceptable viewing solid angle. The mean exit velocities are the same for figures 3, 4, and 5 with the exit temperatures being $1600^{O}K$, $800^{O}K$, and $100^{O}K$ respectively.

When one compares figures 3, 4, and 5, the effect of the exit temperatures on the NCD's is clearly seen. Low exit temperatures tend to keep the exit plume from expanding in a direction perpendicular to the mean exit velocity. This is clear from the fact that the NCD's are larger for observation angles above 270^{O} (which are for lines of sight through the exit plume) for the lower temperature cases. This implies that low exit temperatures are important in order to increase the acceptable viewing solid angle around the SS. If one assumes the acceptable value of $1x10^{15}/m^{2}$ for NCD's, then figures 6 and 7 show that any LOS would have unacceptable values for NCD's for a zero mean exit velocity. These zero mean velocity cases could represent a point source leak.

To gain better insight into how the number density function at different positions around the nozzle contributes to the LOS number column densities, equidensity contours as a function of the angle are given in figures 8, 9, and 10 for an exit temperature of $1600^{O}K$ and a mean exit velocity of 4,000m/sec. (Case 1 in Table 1). Figures 11, 12, and 13 are similar plots except the mean exit velocity is 1,000m/sec. (Case 2 in Table 1). Figures 14, 15, and 16 are also a similar set except for a mean exit velocity of 1,000m/sec. and a temperature of $100^{O}K$ (Case 4 in Table 1). Figures 17, 18, and 19 are equidensity plots for zero mean exit velocity (Case 5 in Table 1).

Figures 20, 21, and 22 are presented to show how the equidensity contours are elongated (for a fixed mean exit velocity) as the temperature approaches zero. All three plots show how the gas expands in a direction perpendicular to the mean exit velocity (positive x-axis). Notice the maximum distance (y value) occurs at larger values of x for the lower exit temperatures. These plots are not to imply that CO_2 will remain a gas at these low temperatures as it exits from a real nozzle, but suggests how an ideal gas plume will behave as the temperature approaches zero with this model.

DISCUSSION

If the allowable limit for the NCD's for CO_2 is assumed to be $1x10^{15}$ molecules/m^2, then any observation angle greater than 270^O (parallel to the mean exit velocity vector $\vec{u}$) would be unacceptable for all the cases shown in Table 1. A study of Table 1 and the figures presented reveal, as one might expect from the kinetic theory point of view, the need to have high mean exit velocities at low exit temperatures to confine the plume in such a manner as to maximize the allowable viewing solid angle.

For a mean exit velocity of 2000m/sec. and a temperature of $100^{O}K$, a maximum observation angle limit of 260^{O} is suggested by the data displayed in figure 23. For lines of sight at an observation angle greater than 260^{O}, the NCD's will be greater than $1x10^{15}/m^2$.

TABLE 1

ANGLE (deg) Φ	COLUMN DENSITIES (particles/m^2) CASE 1	CASE 2	CASE 3
0			
30	5.7E+03	1.6E+15	3.4E+14
60	3.0E+03	7.3E+14	1.6E+14
90	2.4E+03	5.4E+14	1.2E+14
120	2.6E+03	5.1E+14	1.1E+14
150	4.0E+03	6.1E+14	1.4E+14
180	1.2E+04	8.5E+14	2.3E+14
210	6.6E+06	2.0E+15	7.8E+14
240	3.8E+12	5.7E+15	4.7E+15
270	1.5E+16	1.5E+16	2.1E+16
300	3.6E+16	2.9E+16	4.6E+16
330	6.3E+16	5.9E+16	8.8E+16
360			

ANGLE (deg) Φ	CASE 4	CASE 5	CASE 6
0			
30	2.3E+04	6.1E+16	8.0E+16
60	1.2E+04	2.8E+16	3.5E+16
90	9.8E+03	1.8E+16	2.3E+16
120	1.1E+04	1.4E+16	1.7E+16
150	1.6E+04	1.2E+16	1.5E+16
180	4.9E+04	1.0E+16	1.3E+16
210	2.7E+07	1.2E+16	1.5E+16
240	1.5E+13	1.4E+16	1.7E+16
270	5.8E+16	1.8E+16	2.3E+16
300	1.5E+17	2.8E+16	3.5E+16
330	2.6E+17	6.1E+16	8.0E+16
360			

CASE 1: (CO_2), TEMPERATURE 1600 K, VELOCITY 4000 M/S.
CASE 2: (CO_2), TEMPERATURE 1600 K, VELOCITY 1000 M/S.
CASE 3: (CO_2), TEMPERATURE 800 K, VELOCITY 1000 M/S.
CASE 4: (CO_2), TEMPERATURE 100 K, VELOCITY 1000 M/S.
CASE 5: (CO_2), TEMPERATURE 300 K, VELOCITY 0 M/S.
CASE 6: (N_2) , TEMPERATURE 300 K, VELOCITY 0 M/S.

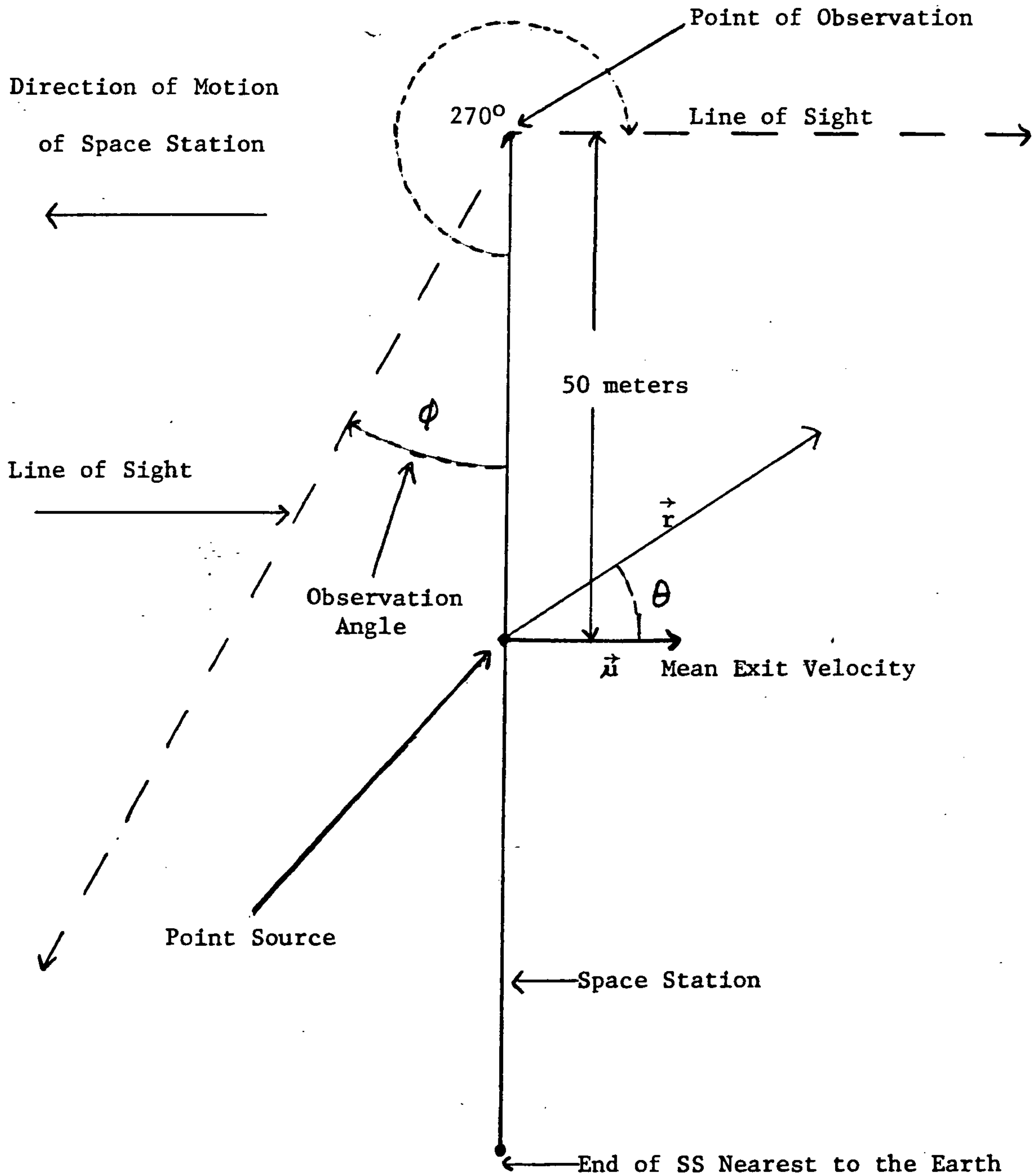

Point of Observation
Direction of Motion
of Space Station
270°
Line of Sight
50 meters
Φ
Line of Sight
r
θ
Observation
Angle
u
Mean Exit Velocity
Point Source
Space Station
End of SS Nearest to the Earth

Figure 1

FIGURE 2

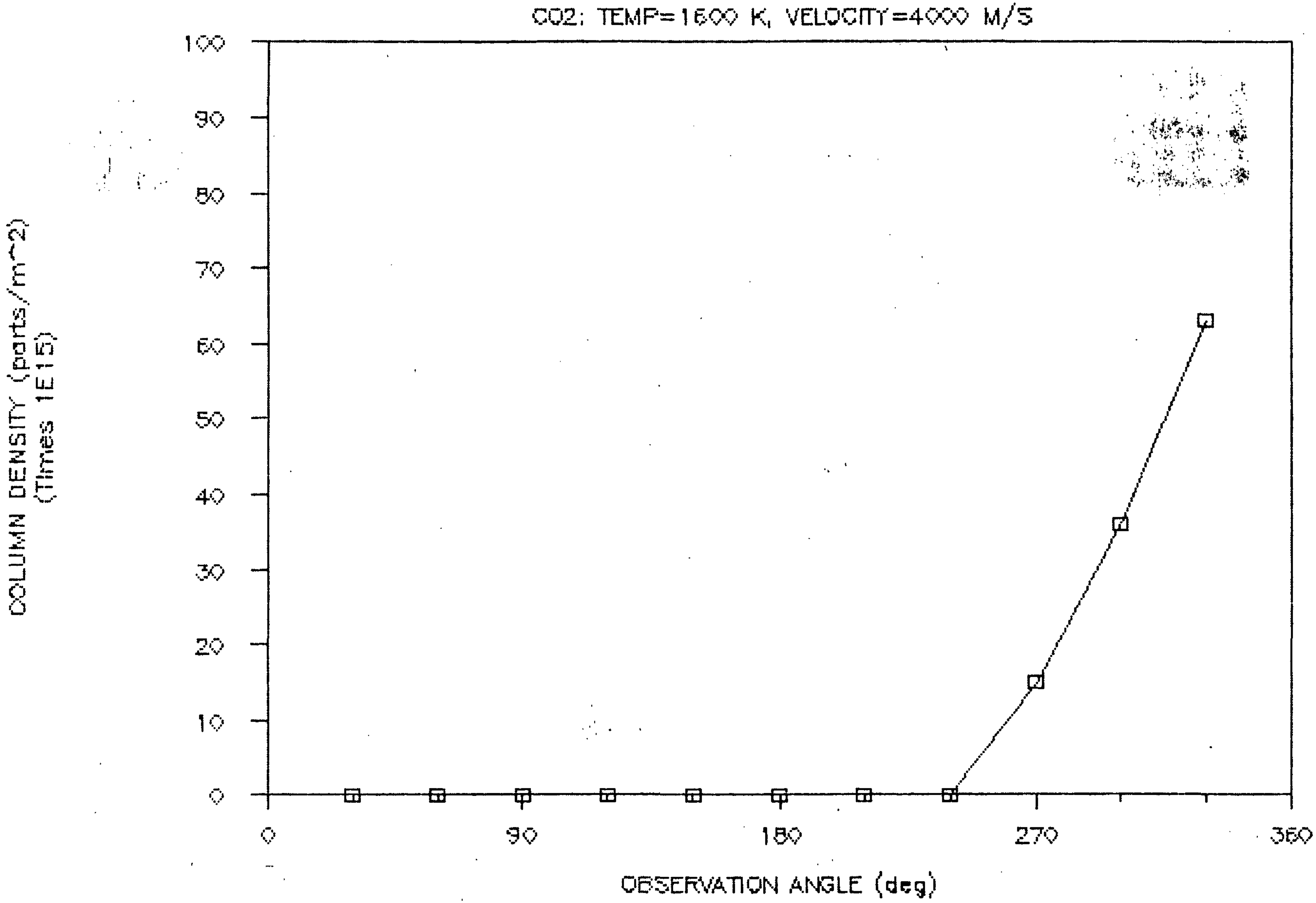
CO2: TEMP=1600 K, VELOCITY=4000 M/S
COLUMN DENSITY (parts/m^2)
(Times 1E15)
0
10
20
30
40
50
60
70
80
90
100
0
90
180
270
360
OBSERVATION ANGLE (deg)

FIGURE 3

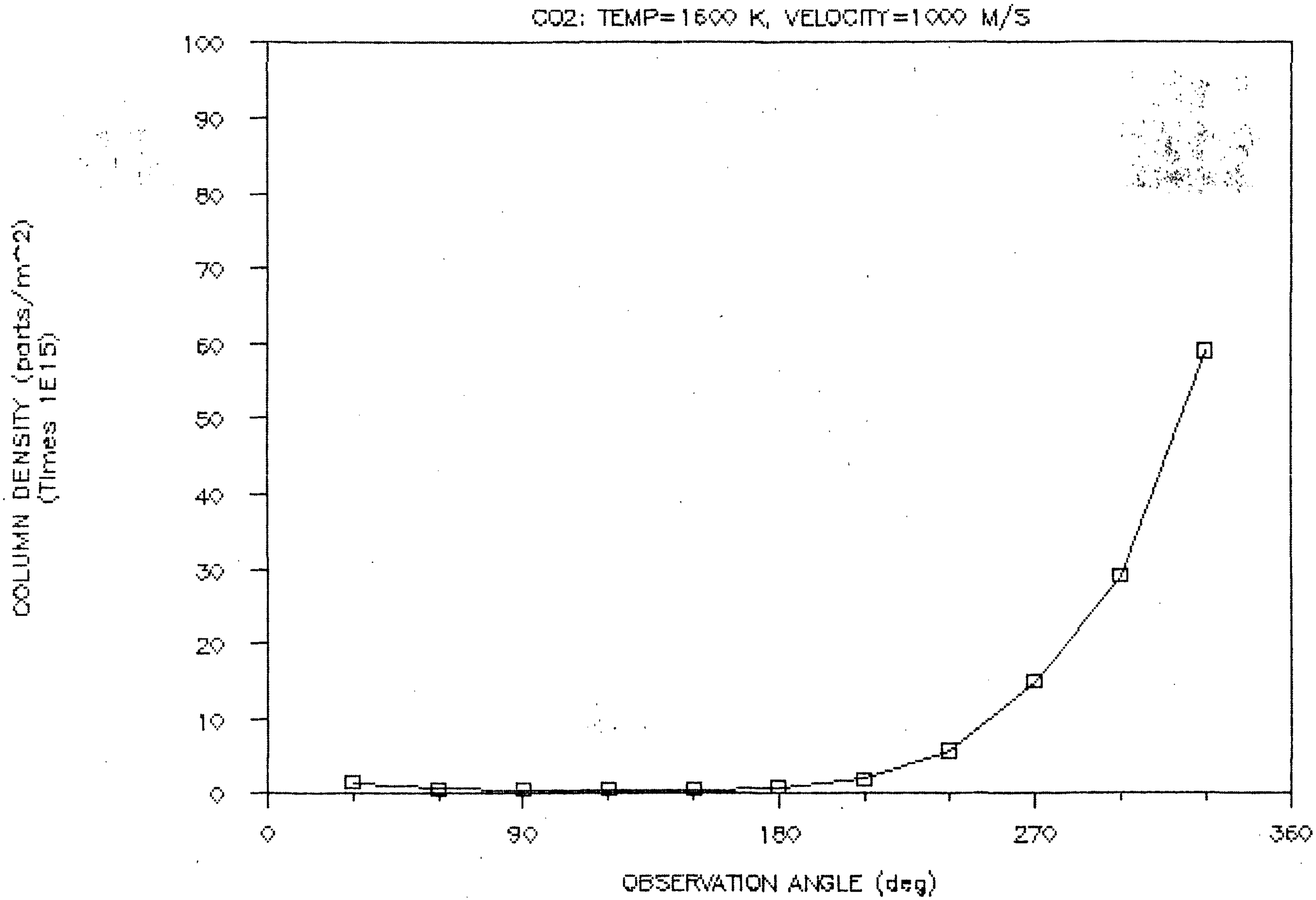
CO2: TEMP=1600 K, VELOCITY=1000 M/S
100
90
80
70
60
50
40
30
20
10
0
0
90
180
270
360
COLUMN DENSITY (parts/m^2)
(Times 1E15)
OBSERVATION ANGLE (deg)

FIGURE 4

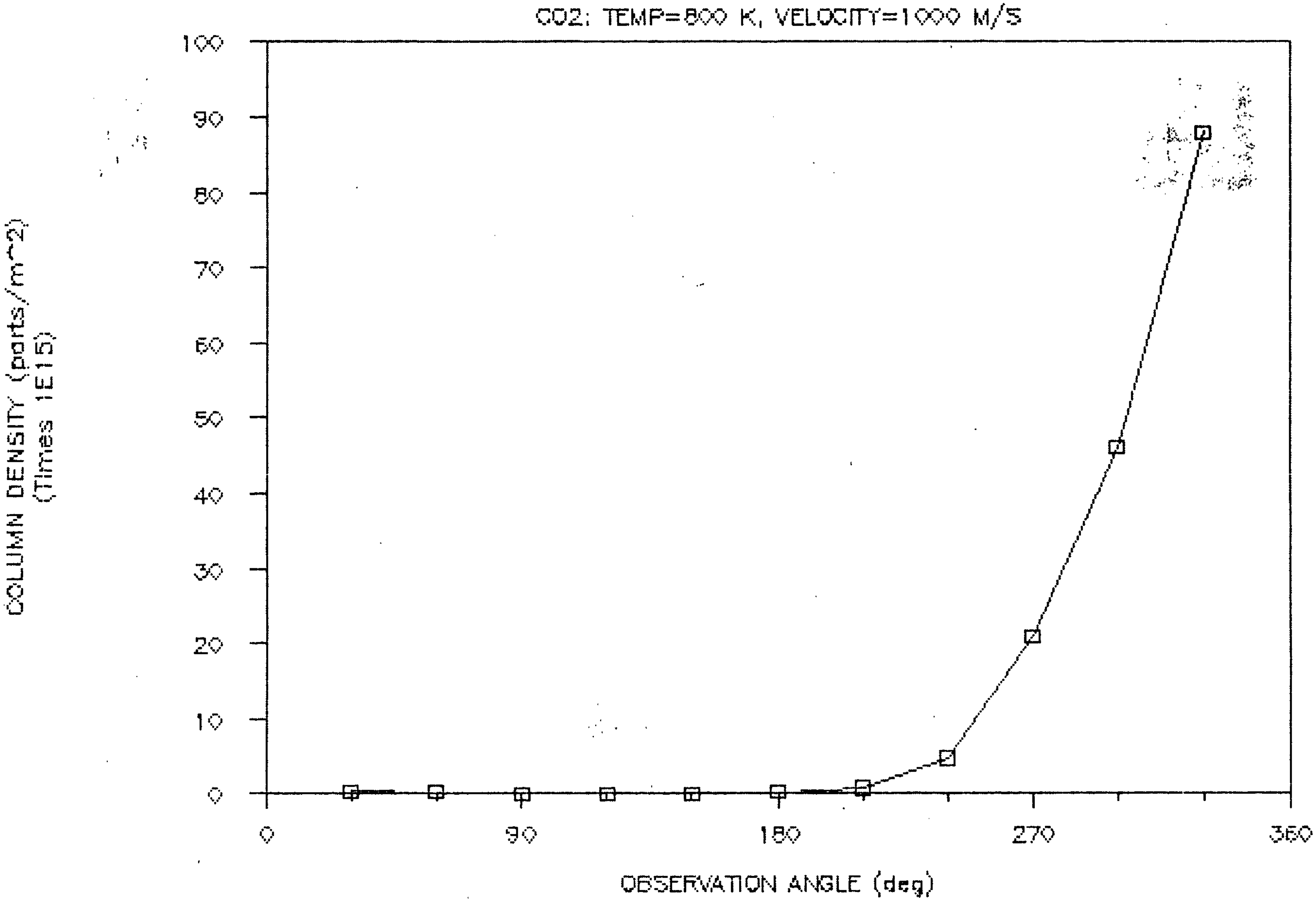
CO2: TEMP=800 K, VELOCITY=1000 M/S
COLUMN DENSITY (parts/m^2)
(Times 1E15)
0
10
20
30
40
50
60
70
80
90
100
0
90
180
270
360
OBSERVATION ANGLE (deg)

FIGURE 5

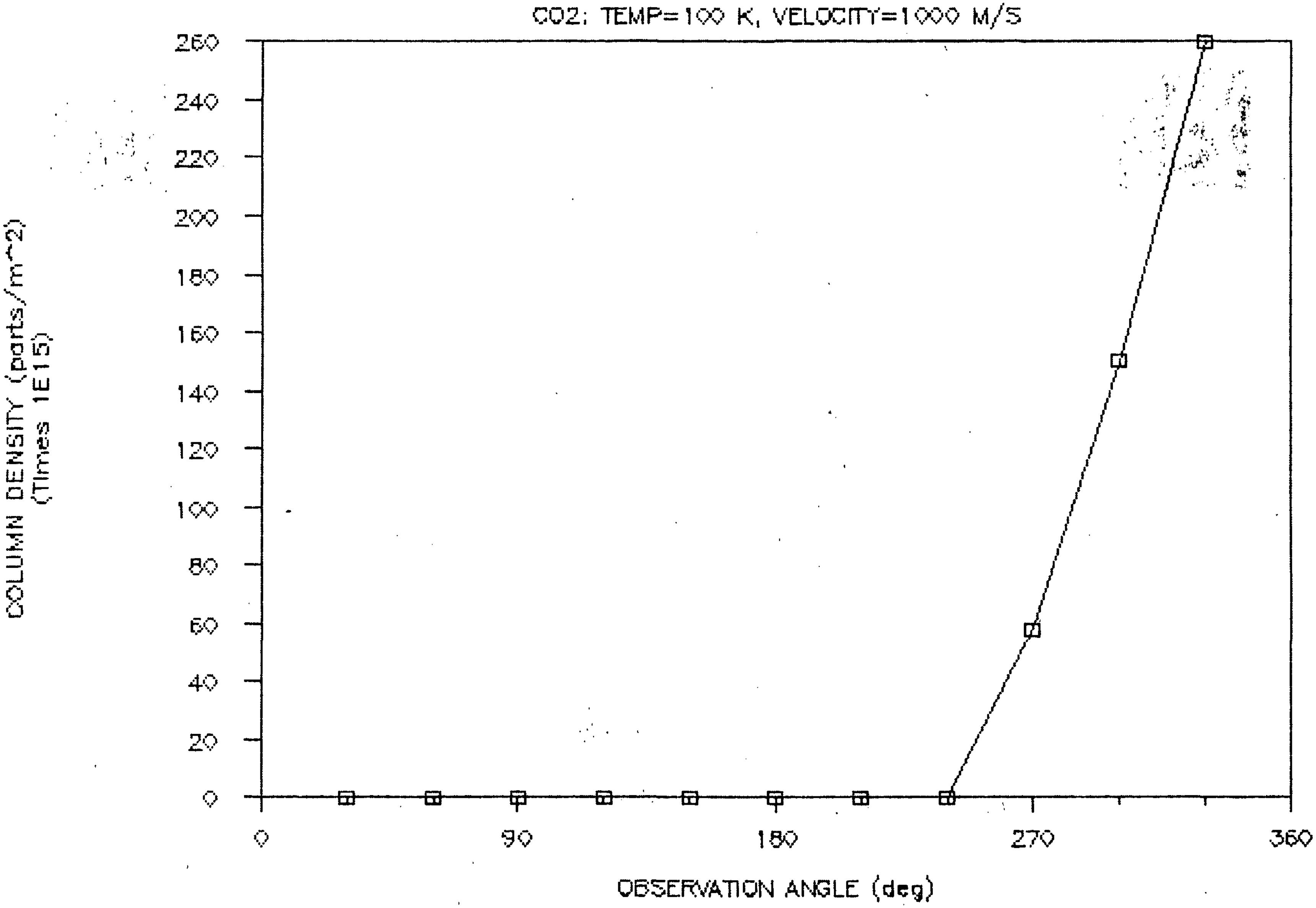
CO2: TEMP=100 K, VELOCITY=1000 M/S
COLUMN DENSITY (parts/m^2)
(Times 1E15)
260
240
220
200
180
160
140
120
100
80
60
40
20
0
0
90
180
270
360
OBSERVATION ANGLE (deg)

FIGURE 6

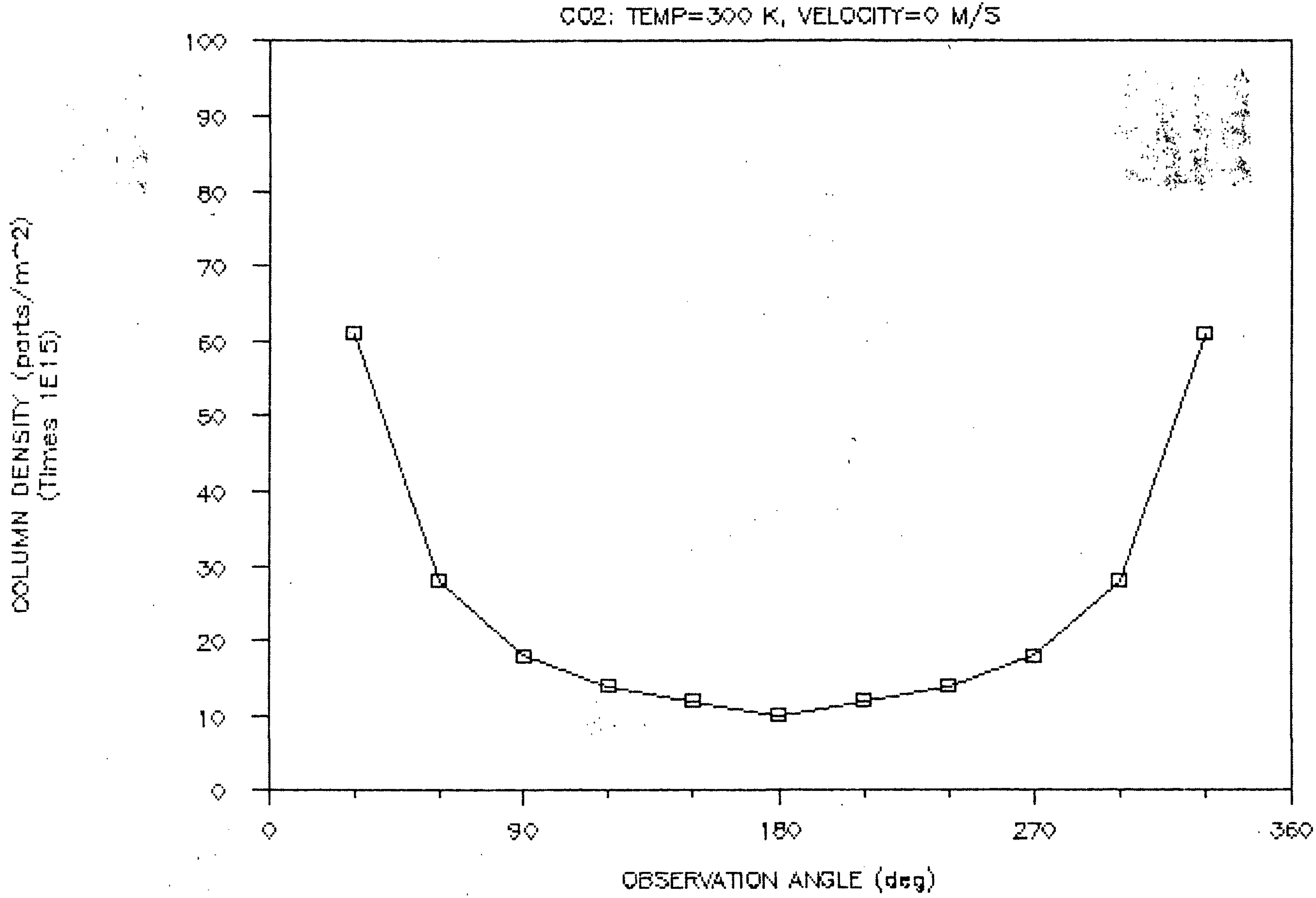
CO2: TEMP=300 K, VELOCITY=0 M/S
COLUMN DENSITY (parts/m^2)
(Times 1E15)
100
90
80
70
60
50
40
30
20
10
0
0
90
180
270
360
OBSERVATION ANGLE (deg)

FIGURE 7

N2: TEMP=300 K, VELOCITY=0 M/S

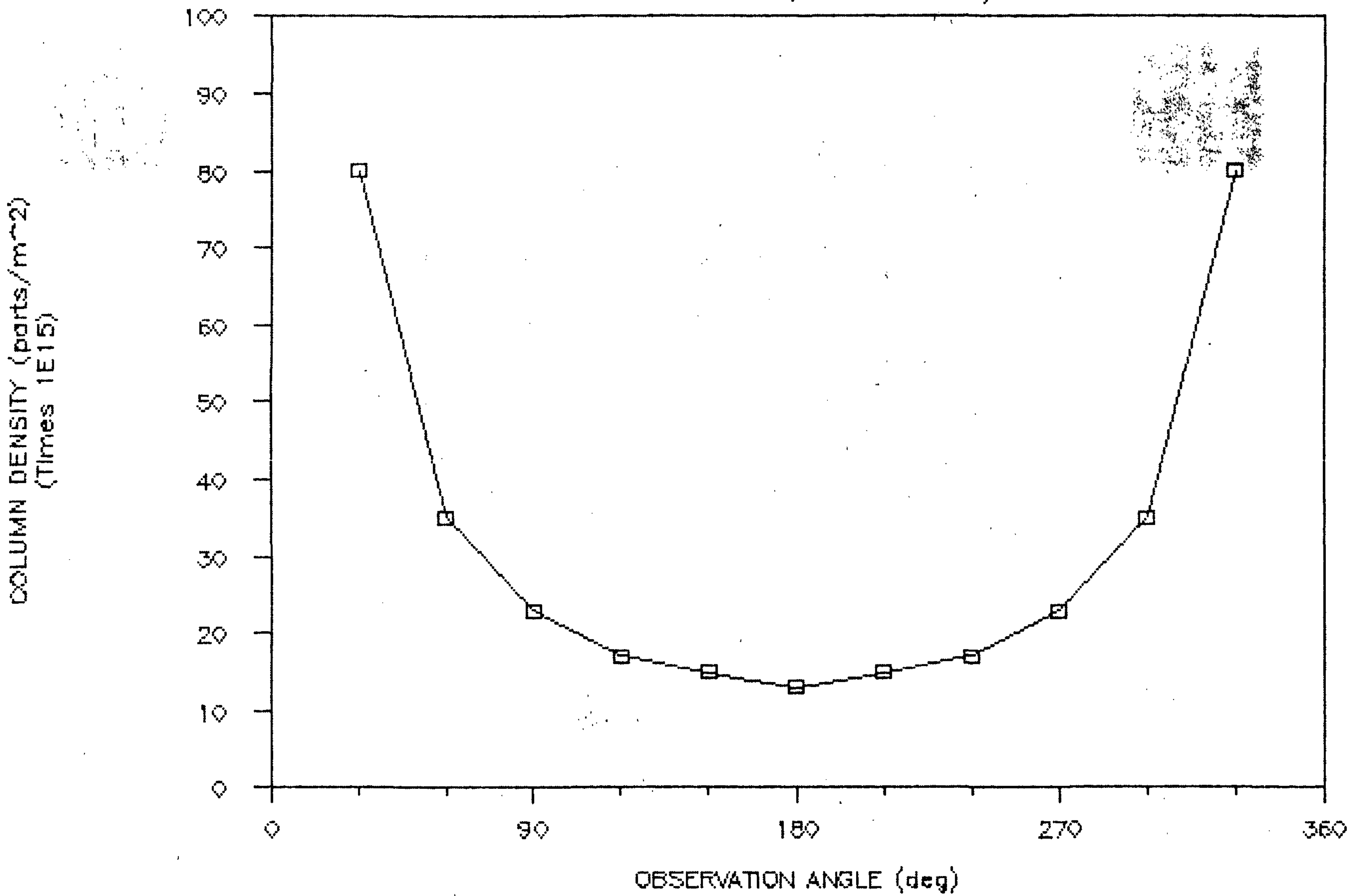

FIGURE 8

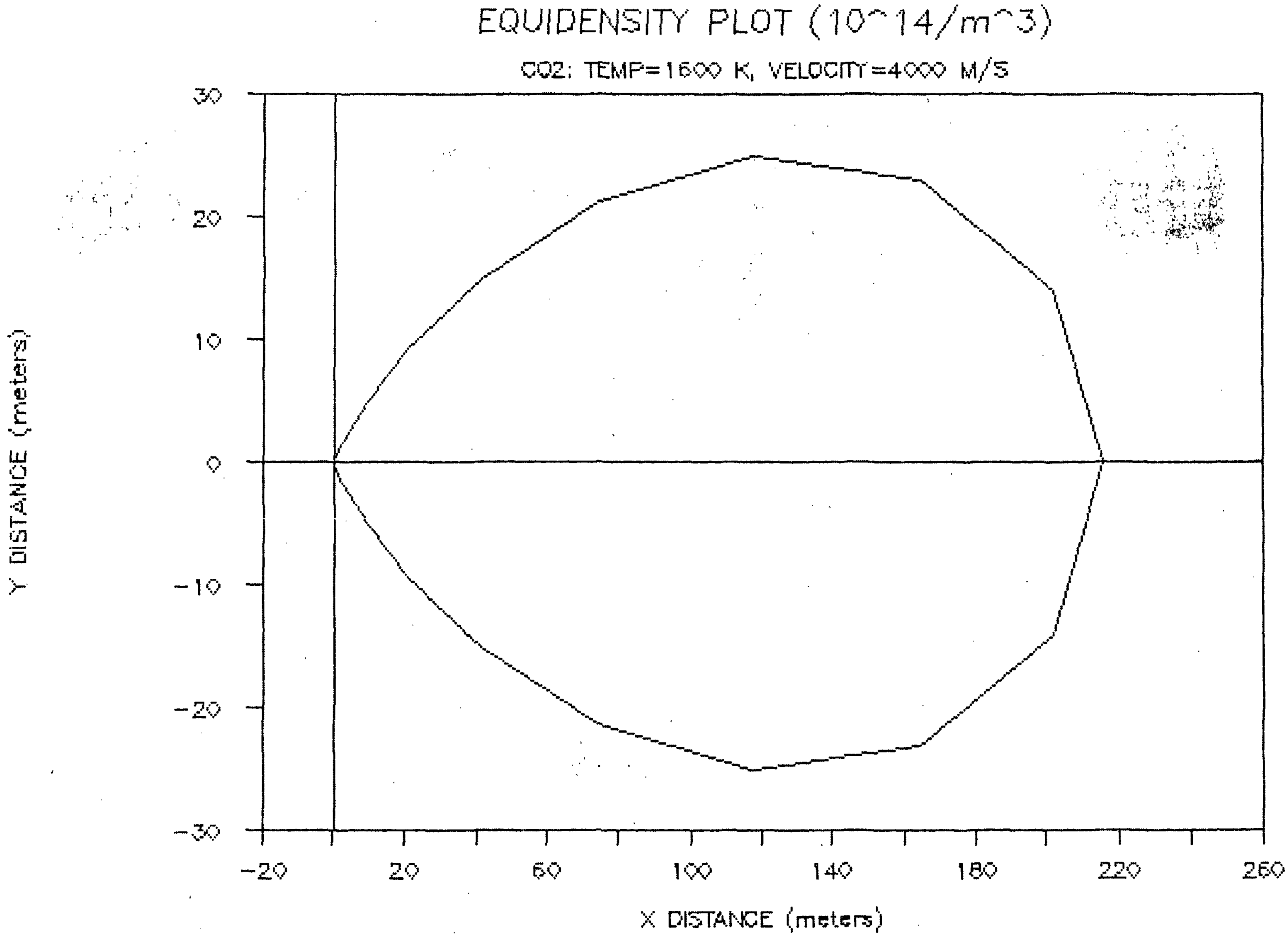
EQUIDENSITY PLOT (10^14/m^3)
CO2: TEMP=1600 K, VELOCITY=4000 M/S
30
20
10
0
-10
-20
-30
-20
20
60
100
140
180
220
260
X DISTANCE (meters)
Y DISTANCE (meters)

FIGURE 9

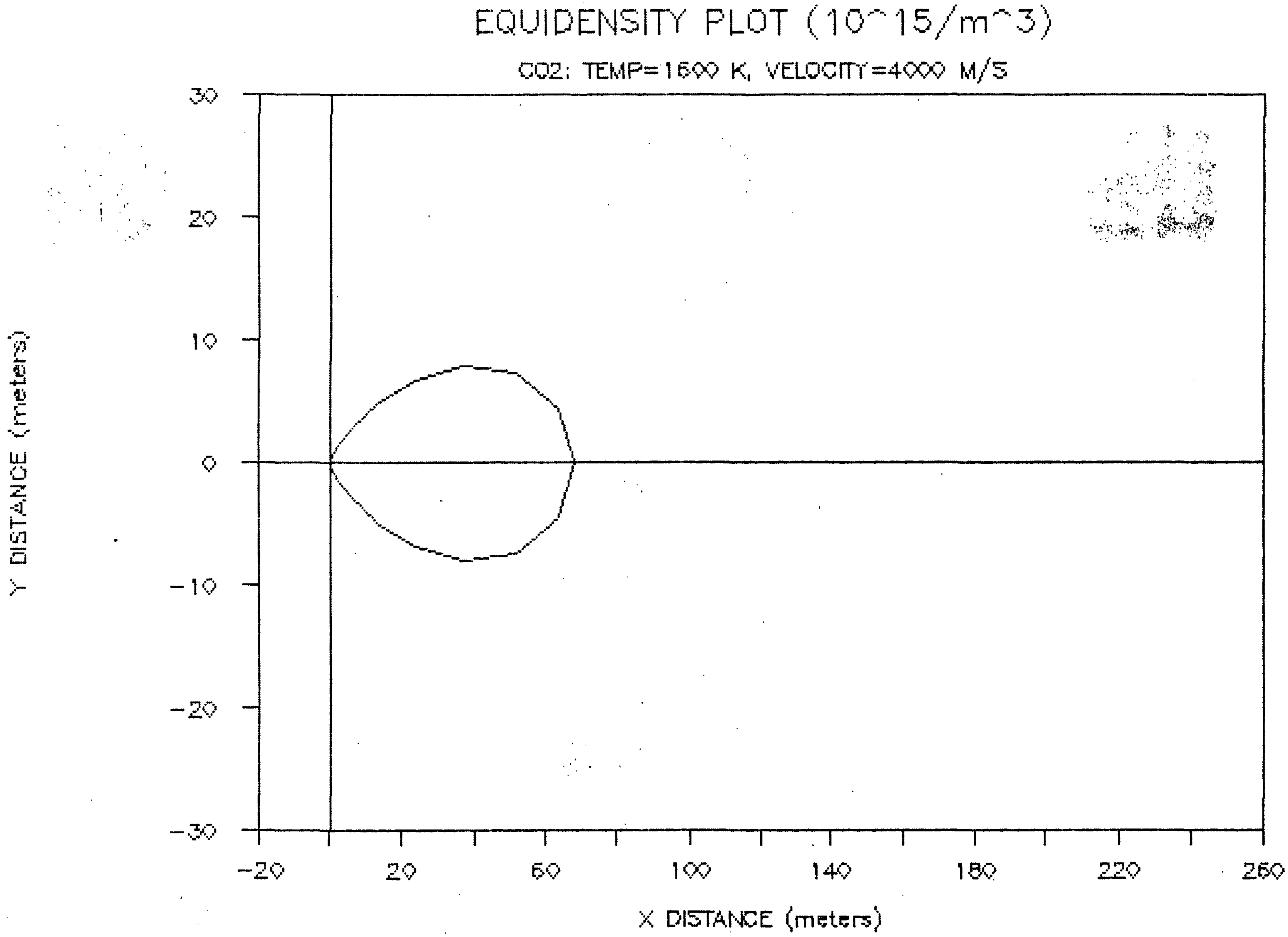
EQUIDENSITY PLOT (10^15/m^3)
CO2: TEMP=1600 K, VELOCITY=4000 M/S
30
20
10
0
-10
-20
-30
-20
20
60
100
140
180
220
260
Y DISTANCE (meters)
X DISTANCE (meters)

FIGURE 10

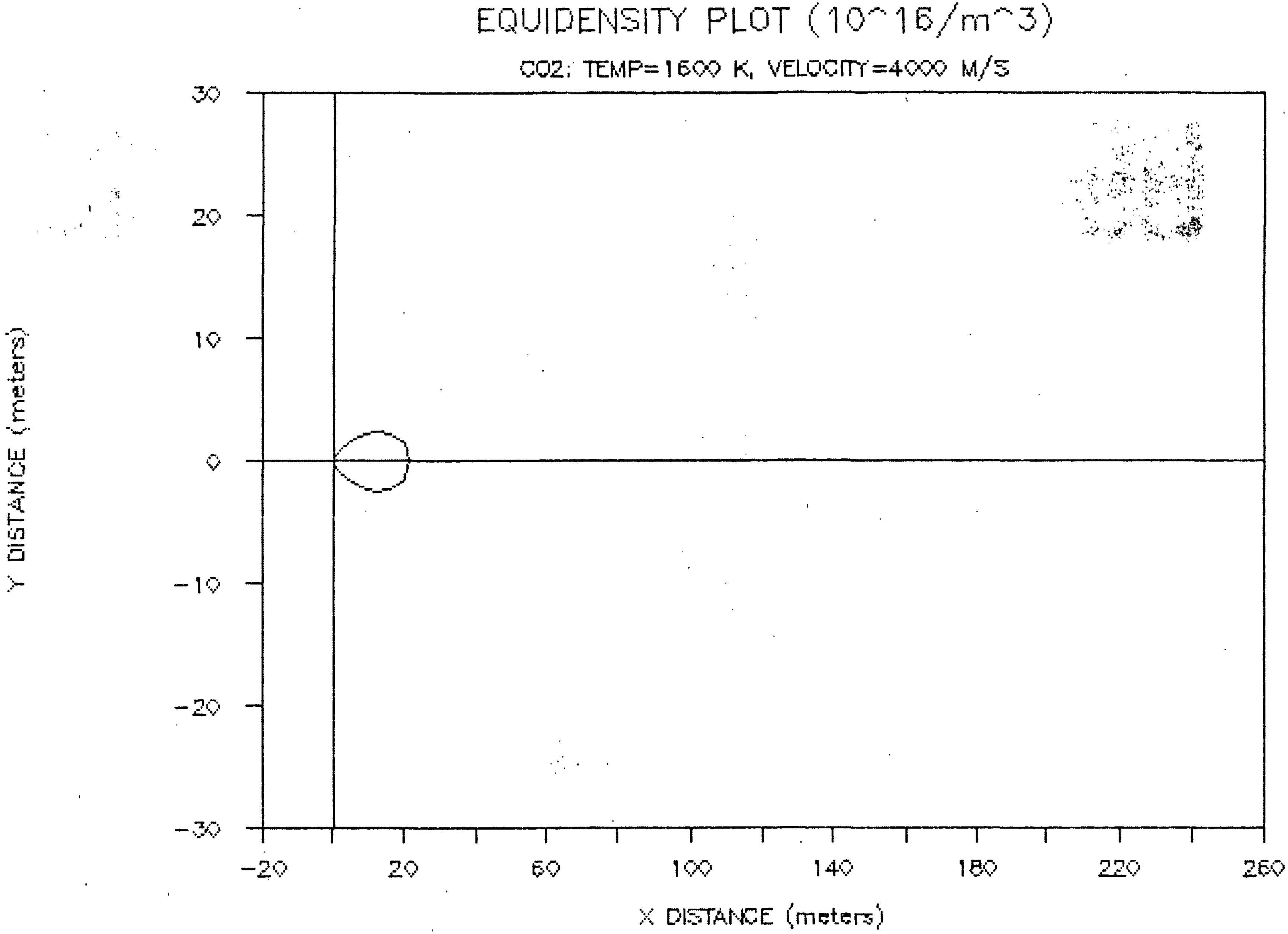
EQUIDENSITY PLOT (10^16/m^3)
CO2: TEMP=1600 K, VELOCITY=4000 M/S
30
20
10
0
−10
−20
−30
Y DISTANCE (meters)
−20
20
60
100
140
180
220
260
X DISTANCE (meters)

FIGURE 11

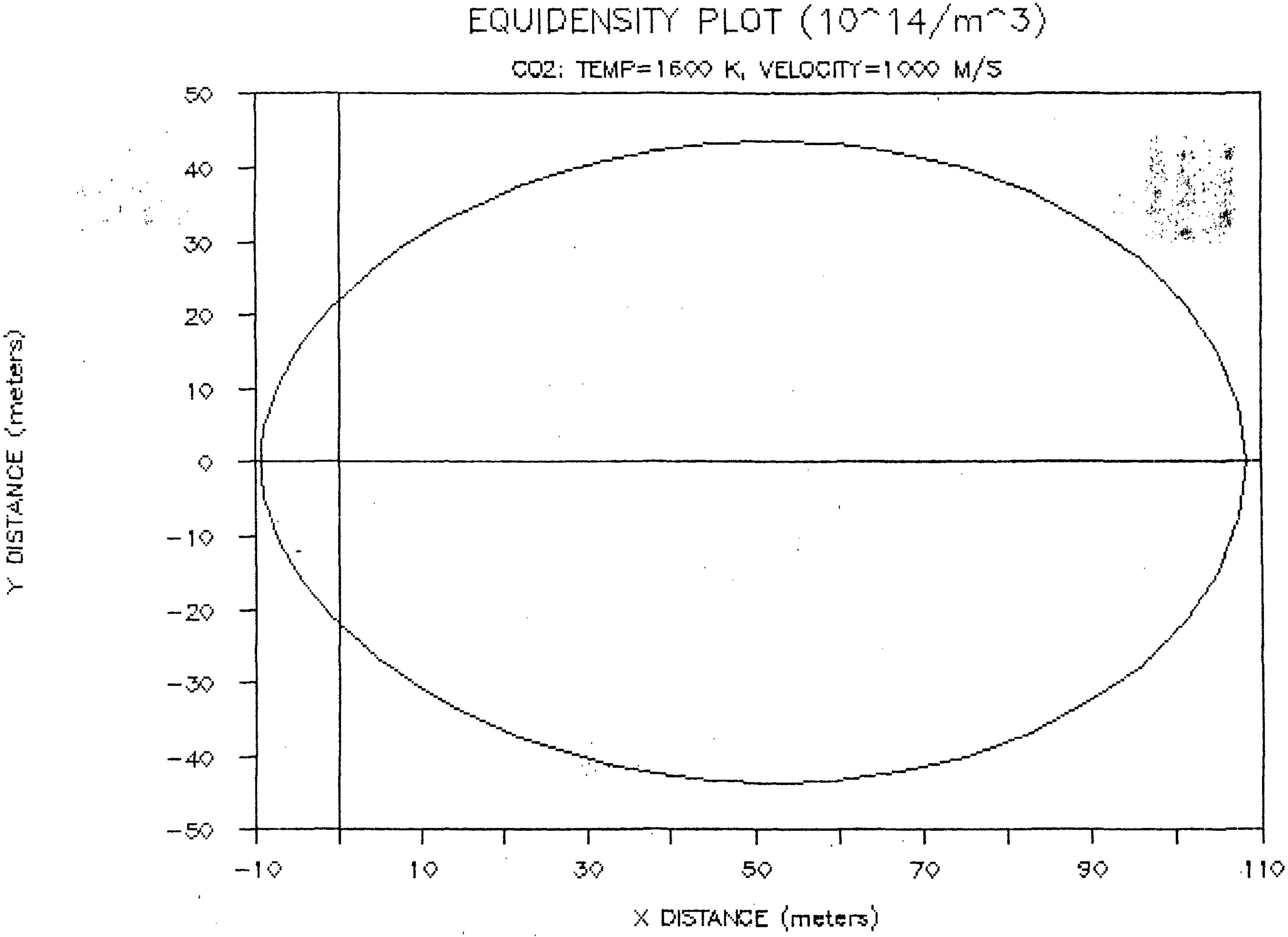
EQUIDENSITY PLOT (10^14/m^3)
CO2: TEMP=1600 K, VELOCITY=1000 M/S
50
40
30
20
10
0
−10
−20
−30
−40
−50
Y DISTANCE (meters)
−10
10
30
50
70
90
110
X DISTANCE (meters)

FIGURE 12

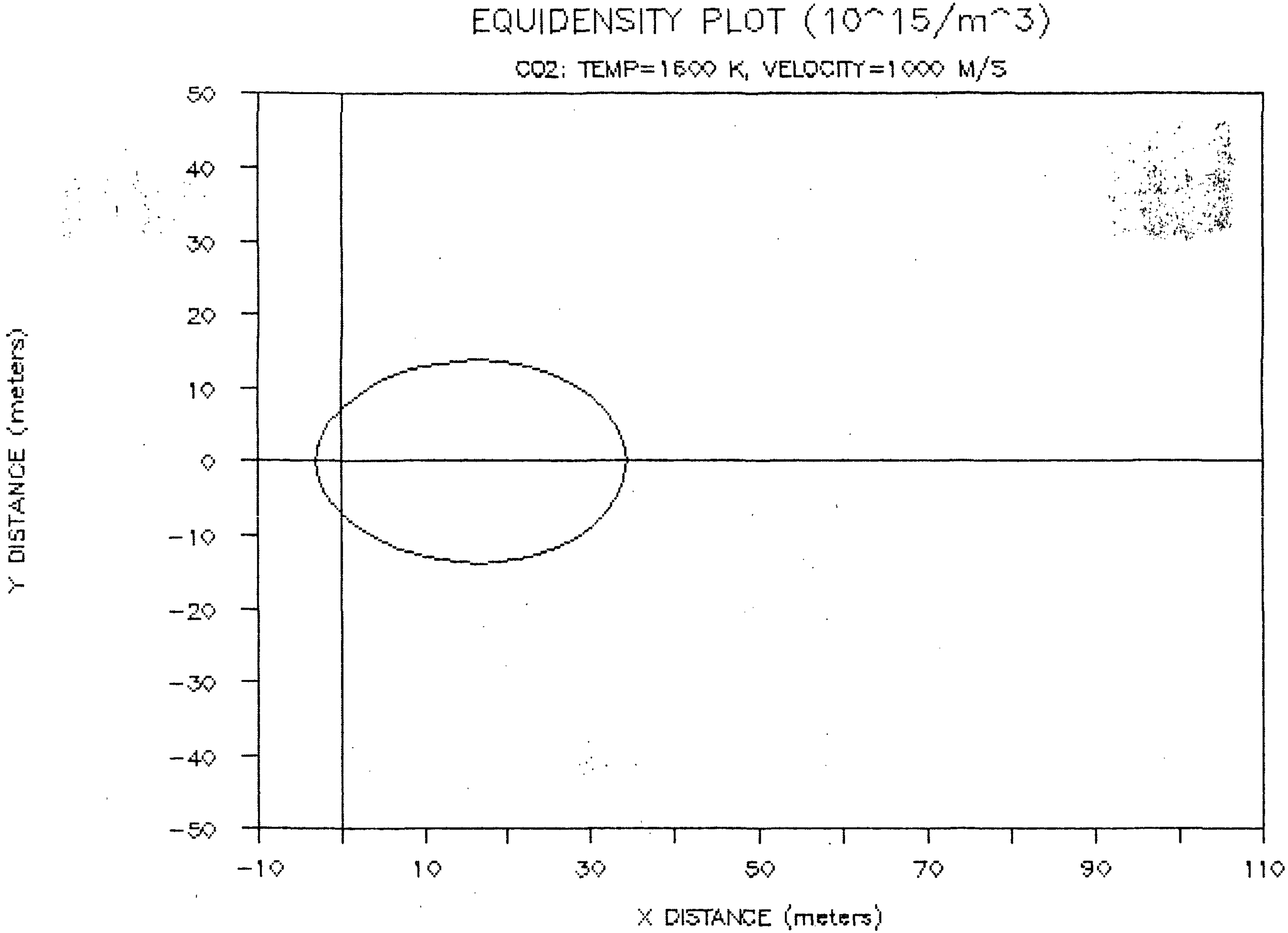
EQUIDENSITY PLOT (10^15/m^3)
CO2: TEMP=1600 K, VELOCITY=1000 M/S
Y DISTANCE (meters)
50
40
30
20
10
0
-10
-20
-30
-40
-50
-10
10
30
50
70
90
110
X DISTANCE (meters)

FIGURE 13

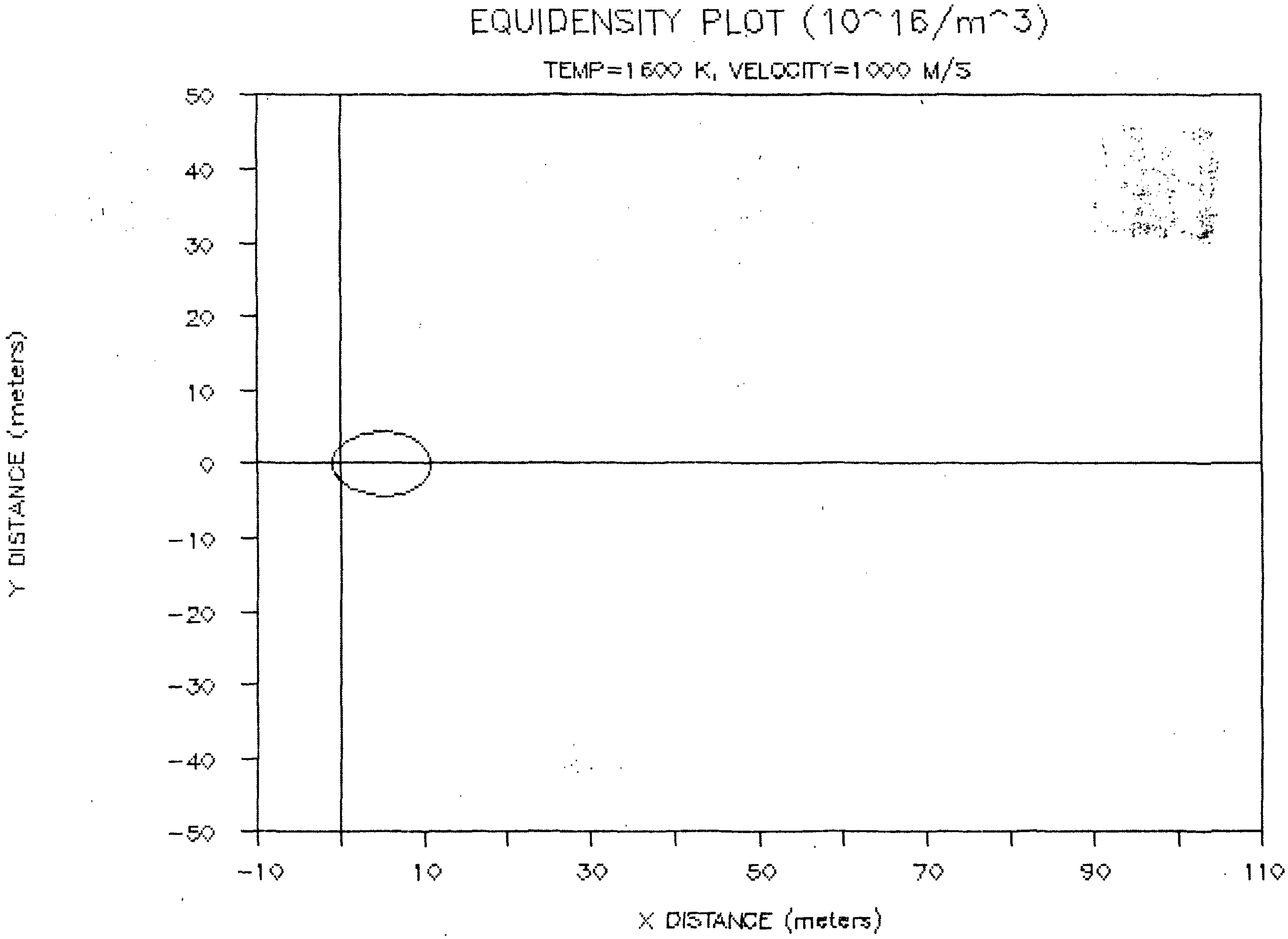
EQUIDENSITY PLOT (10^16/m^3)
TEMP=1600 K, VELOCITY=1000 M/S
Y DISTANCE (meters)
X DISTANCE (meters)
50
40
30
20
10
0
-10
-20
-30
-40
-50
-10
10
30
50
70
90
110

FIGURE 14

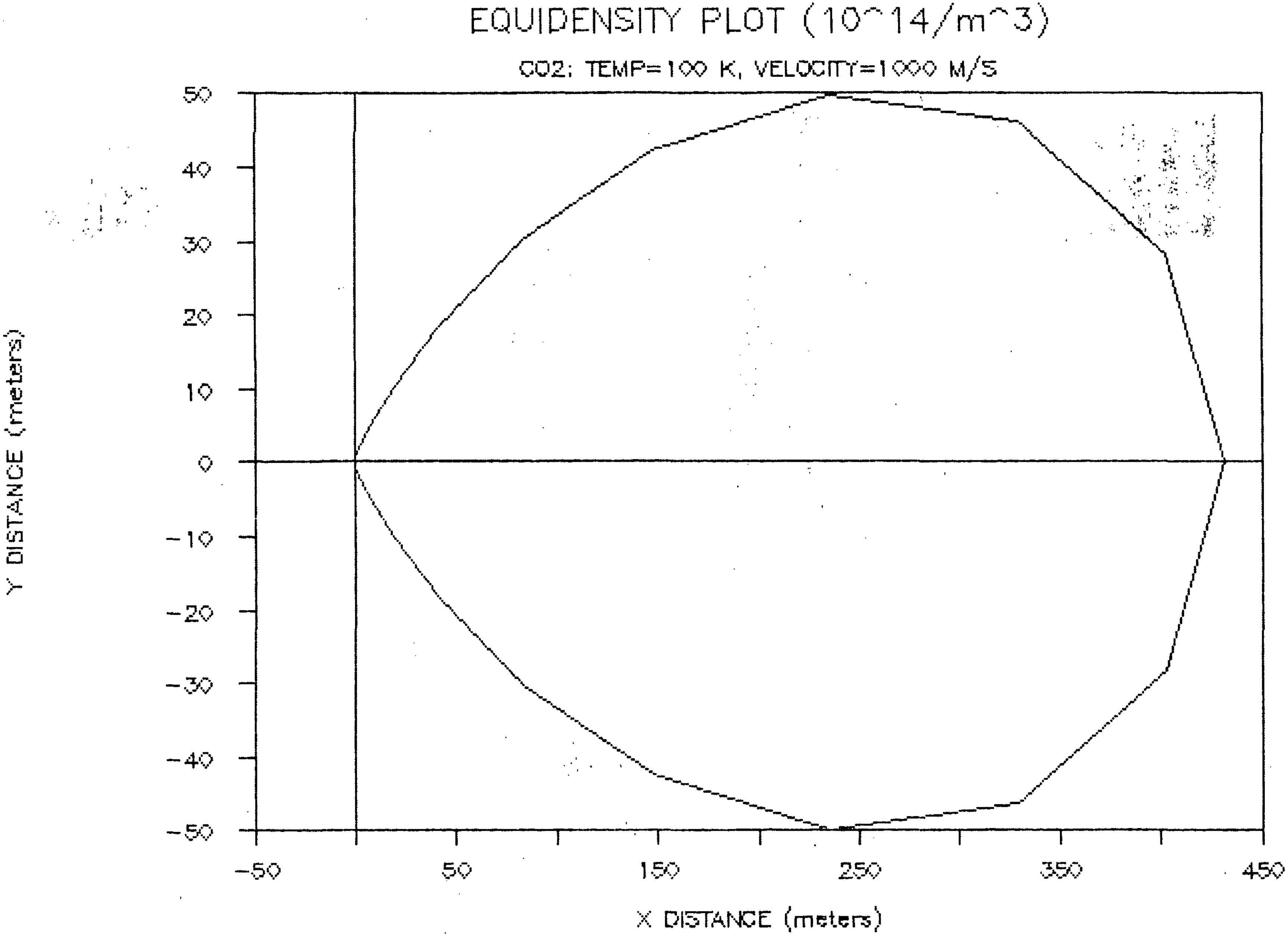
EQUIDENSITY PLOT (10^14/m^3)
CO2: TEMP=100 K, VELOCITY=1000 M/S
Y DISTANCE (meters)
50
40
30
20
10
0
-10
-20
-30
-40
-50
-50
50
150
250
350
450
X DISTANCE (meters)

FIGURE 15

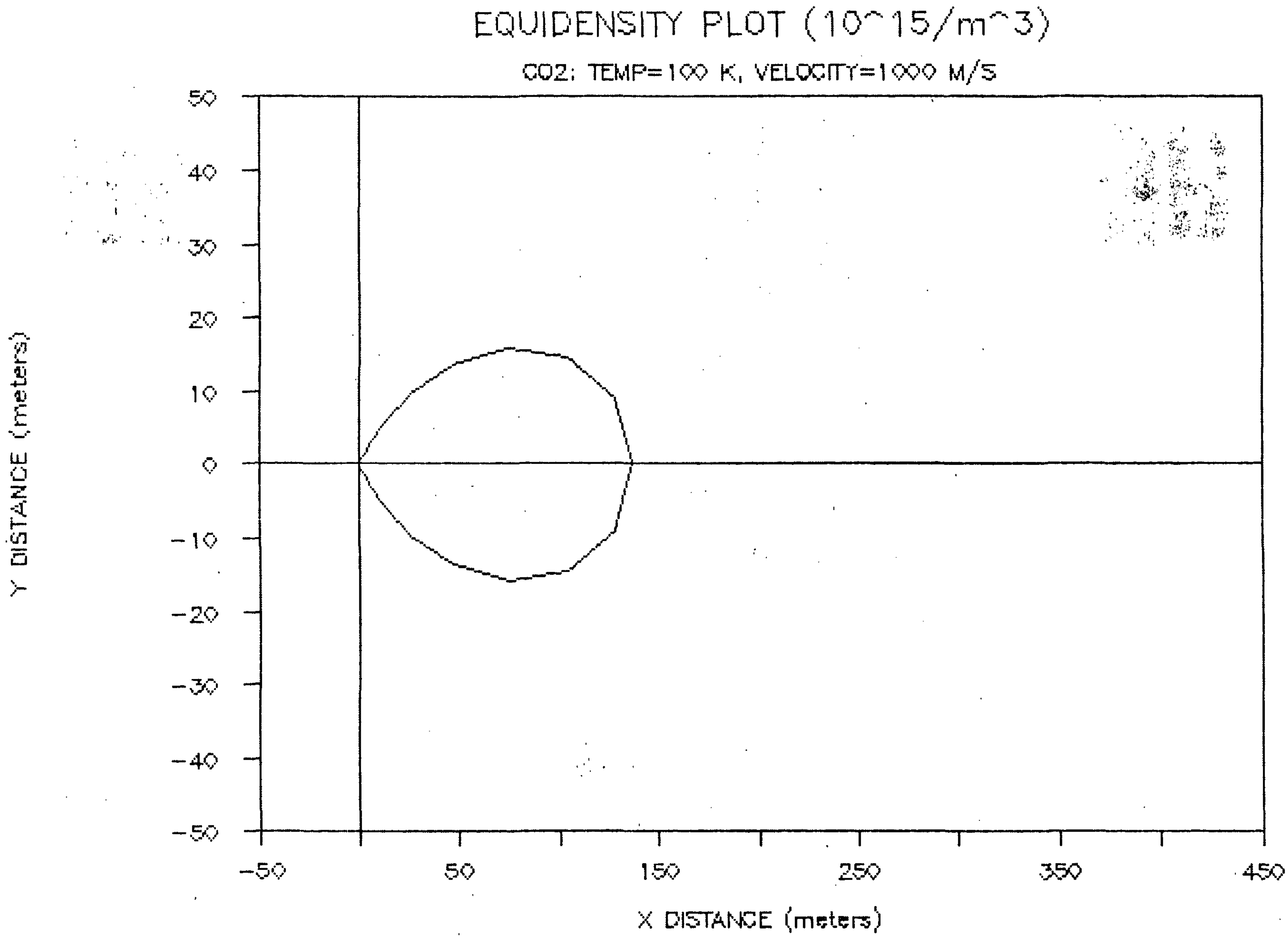
EQUIDENSITY PLOT (10^15/m^3)
CO2: TEMP=100 K, VELOCITY=1000 M/S
50
40
30
20
10
0
-10
-20
-30
-40
-50
Y DISTANCE (meters)
-50
50
150
250
350
450
X DISTANCE (meters)

FIGURE 16

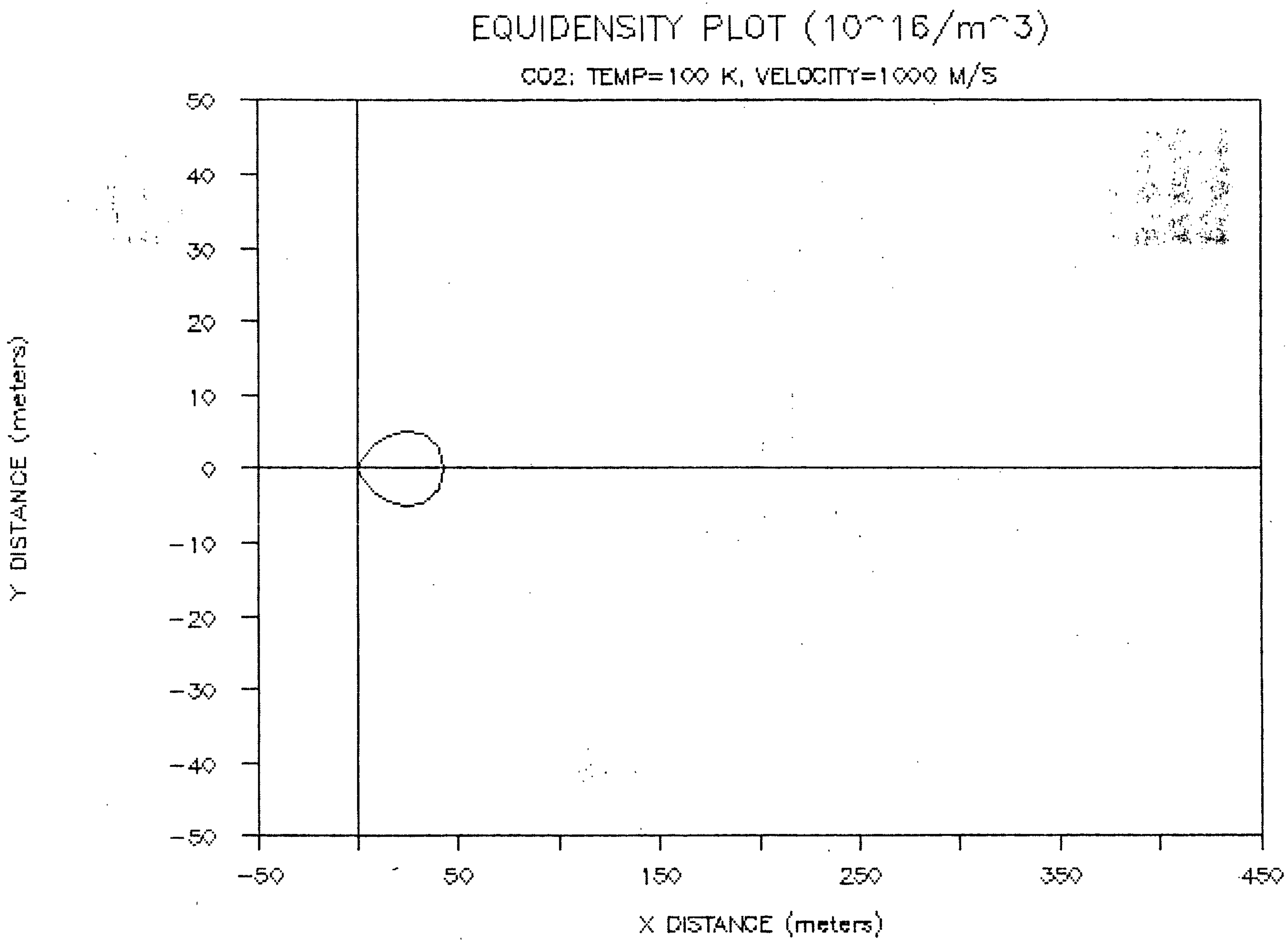
EQUIDENSITY PLOT (10^16/m^3)
CO2: TEMP=100 K, VELOCITY=1000 M/S
Y DISTANCE (meters)
50
40
30
20
10
0
−10
−20
−30
−40
−50
−50
50
150
250
350
450
X DISTANCE (meters)

FIGURE 17

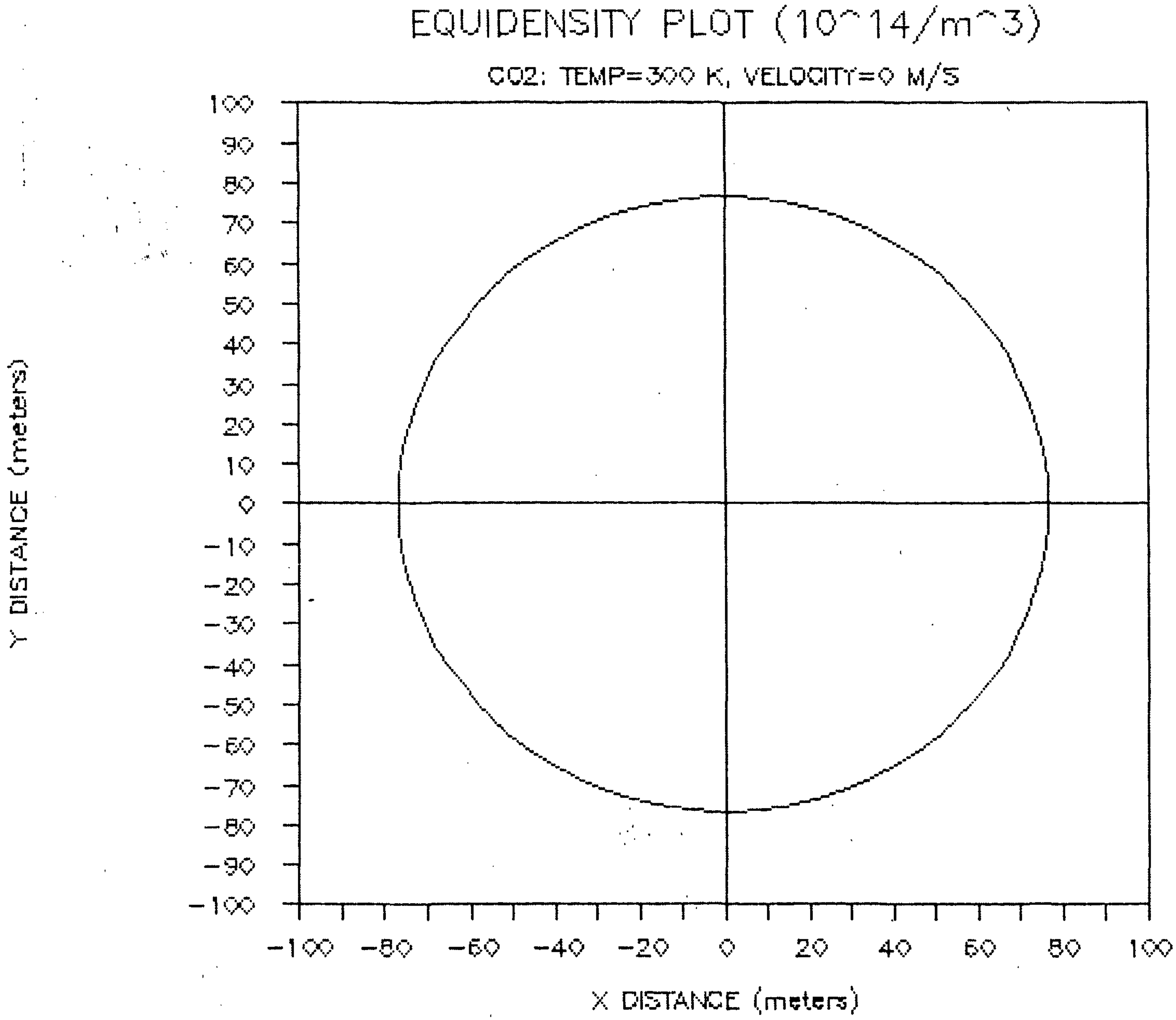
EQUIDENSITY PLOT (10^14/m^3)
CO2: TEMP=300 K, VELOCITY=0 M/S
Y DISTANCE (meters)
100
90
80
70
60
50
40
30
20
10
0
-10
-20
-30
-40
-50
-60
-70
-80
-90
-100
-100 -80 -60 -40 -20 0 20 40 60 80 100
X DISTANCE (meters)

FIGURE 18

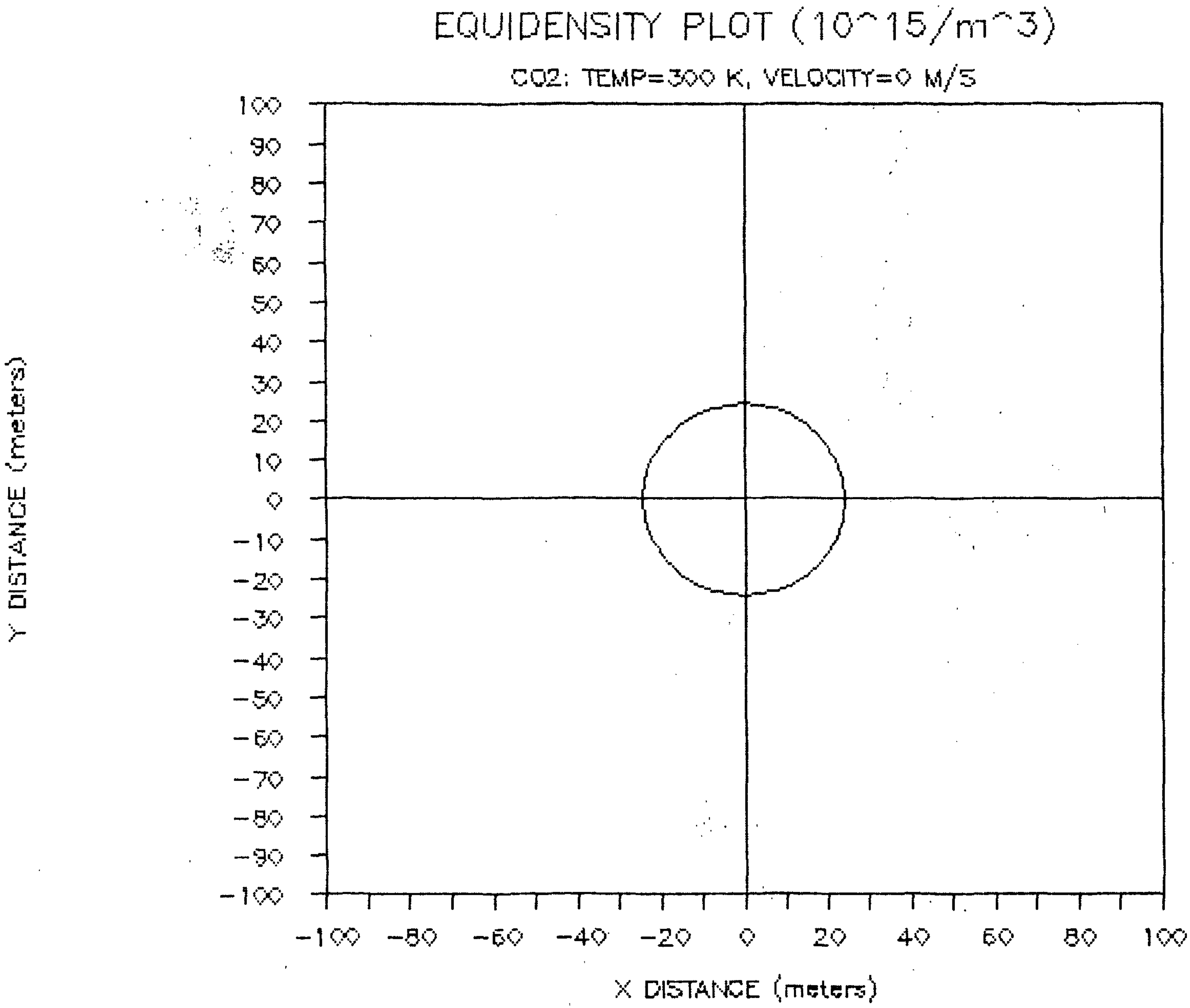
EQUIDENSITY PLOT (10^15/m^3)
CO2: TEMP=300 K, VELOCITY=0 M/S
Y DISTANCE (meters)
100
90
80
70
60
50
40
30
20
10
0
-10
-20
-30
-40
-50
-60
-70
-80
-90
-100
-100 -80 -60 -40 -20 0 20 40 60 80 100
X DISTANCE (meters)

FIGURE 19

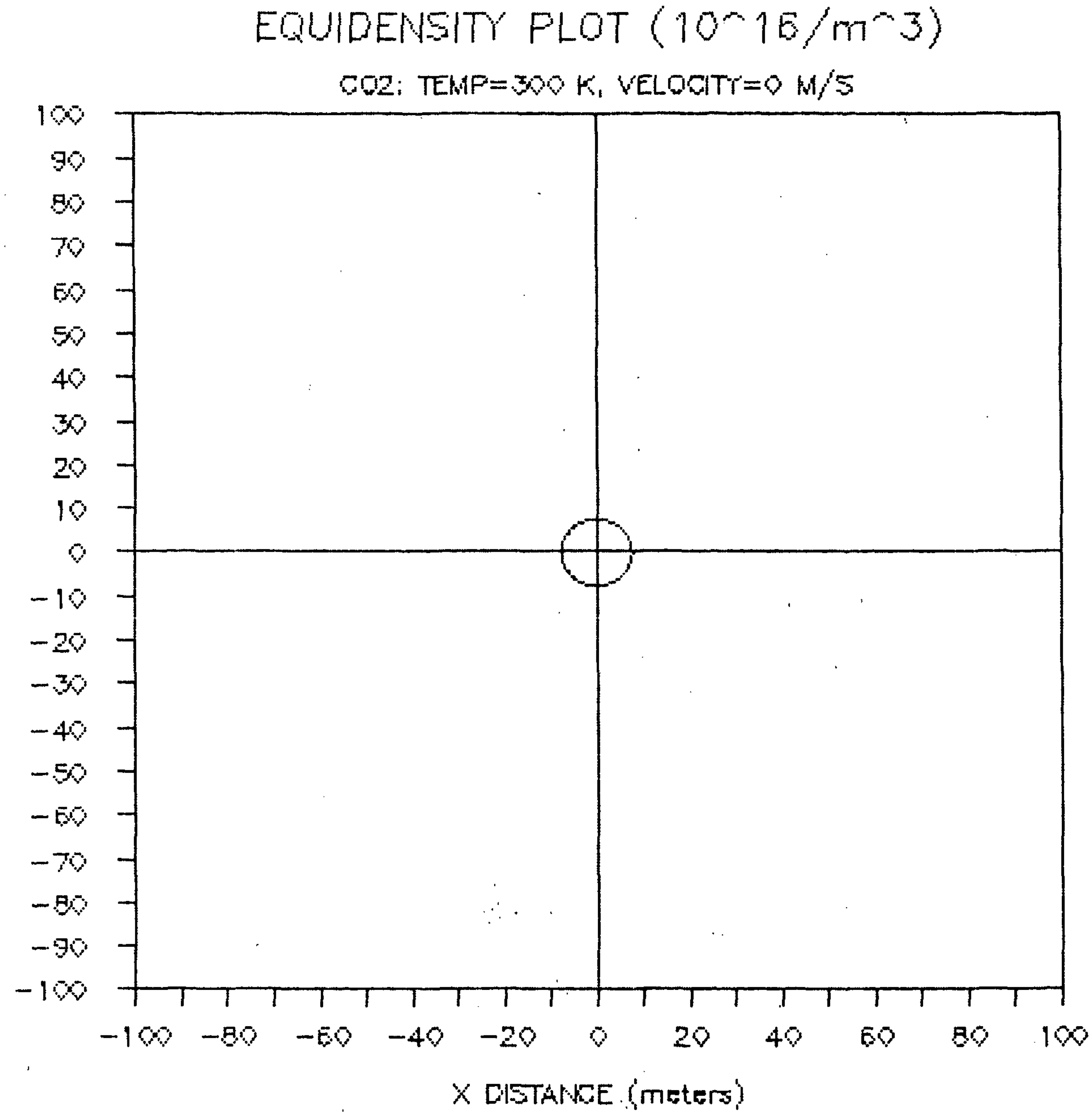

EQUIDENSITY PLOT (10^16/m^3)
CO2: TEMP=300 K, VELOCITY=0 M/S
Y DISTANCE (meters)
X DISTANCE (meters)
100
90
80
70
60
50
40
30
20
10
0
-10
-20
-30
-40
-50
-60
-70
-80
-90
-100
-100 -80 -60 -40 -20 0 20 40 60 80 100

FIGURE 20

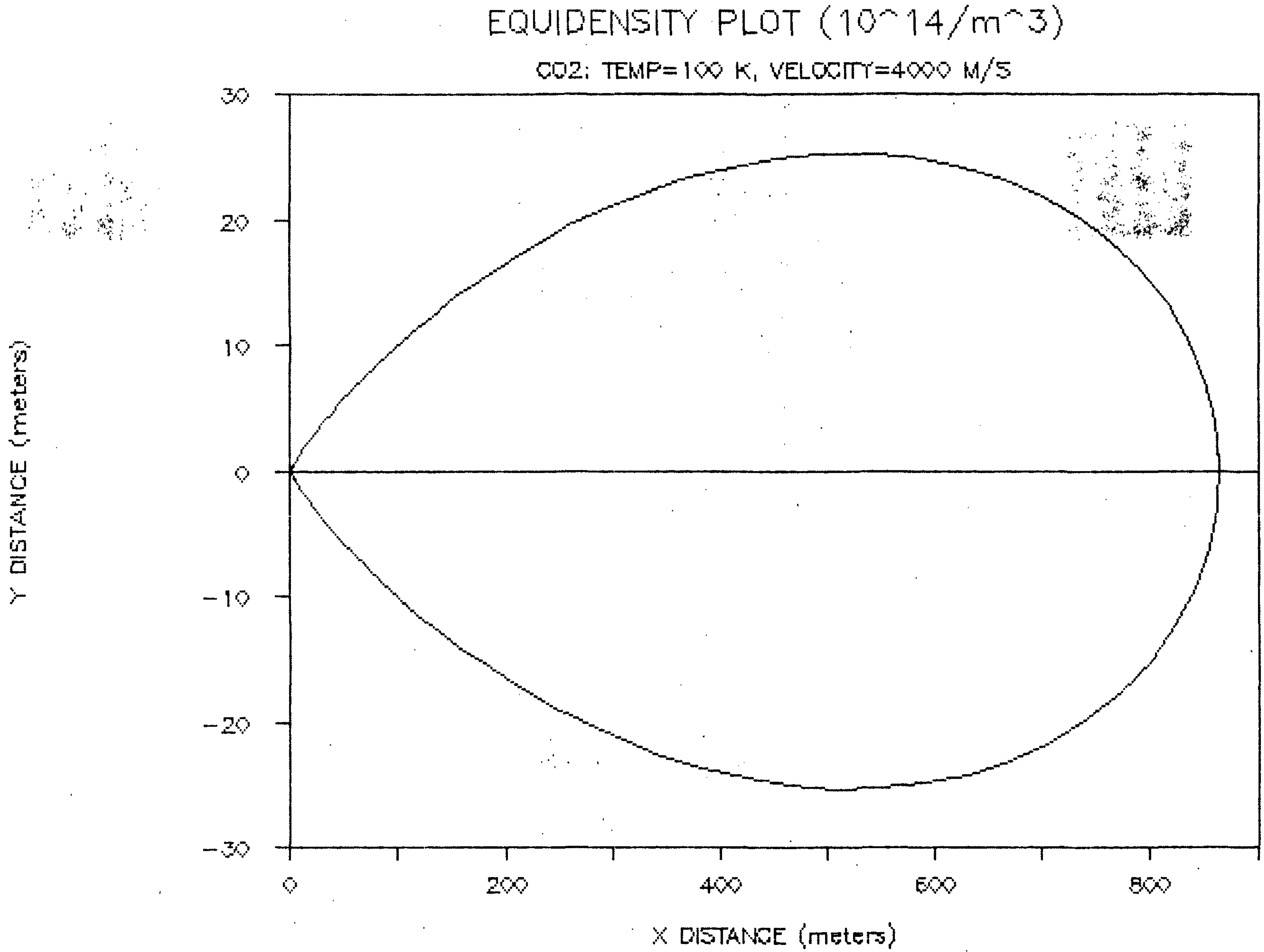

EQUIDENSITY PLOT (10^14/m^3)
CO2; TEMP=100 K, VELOCITY=4000 M/S
30
20
10
0
-10
-20
-30
Y DISTANCE (meters)
0
200
400
600
800
X DISTANCE (meters)

FIGURE 21

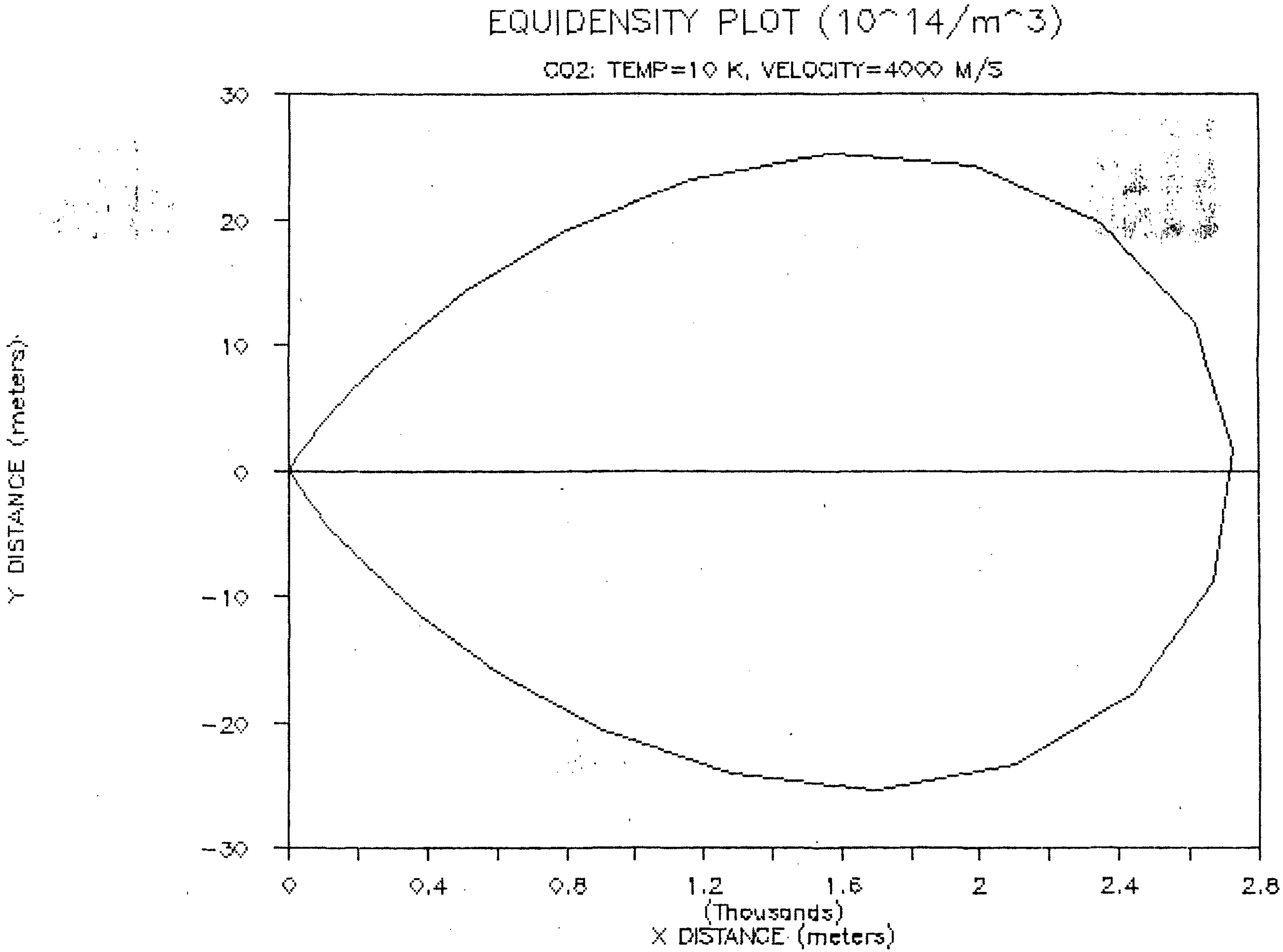
EQUIDENSITY PLOT (10^14/m^3)
CO2: TEMP=10 K, VELOCITY=4000 M/S
30
20
10
0
-10
-20
-30
Y DISTANCE (meters)
0
0.4
0.8
1.2
1.6
2
2.4
2.8
(Thousands)
X DISTANCE (meters)

FIGURE 22

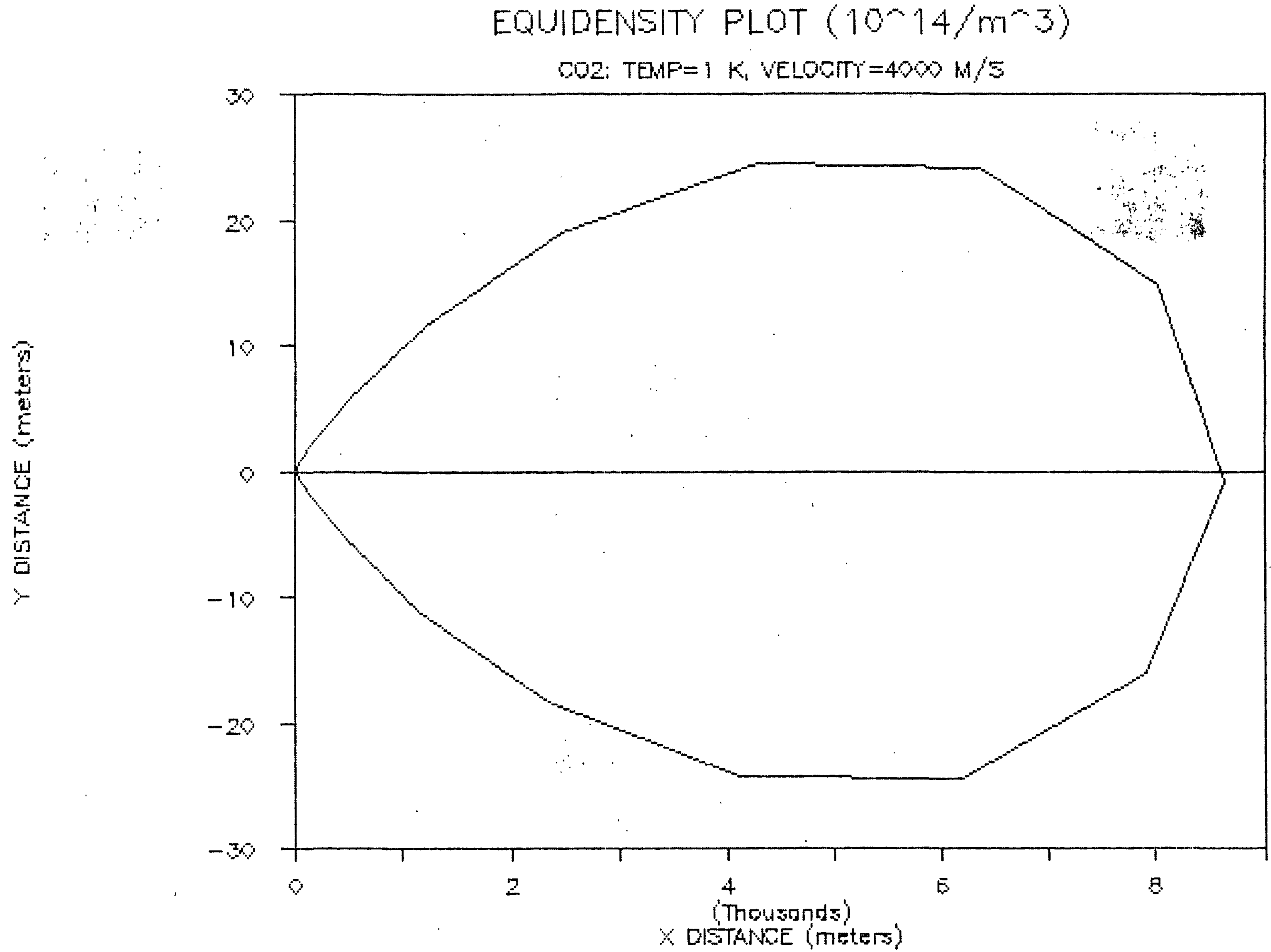

EQUIDENSITY PLOT (10^14/m^3)
CO2: TEMP=1 K, VELOCITY=4000 M/S
Y DISTANCE (meters)
30
20
10
0
-10
-20
-30
0
2
4
6
8
(Thousands)
X DISTANCE (meters)

FIGURE 23

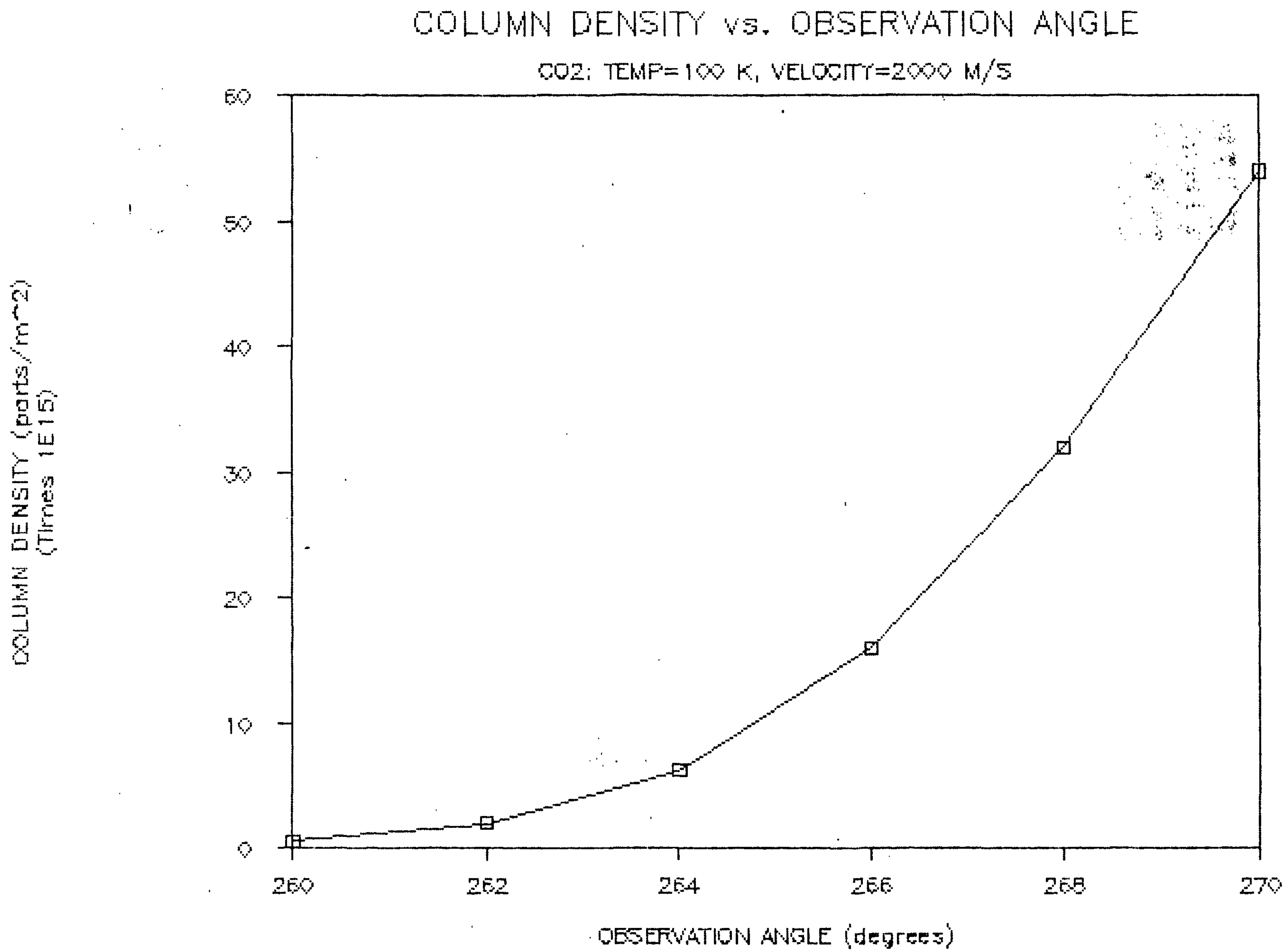
COLUMN DENSITY vs. OBSERVATION ANGLE
CO2: TEMP=100 K, VELOCITY=2000 M/S
COLUMN DENSITY (parts/m^2)
(Times 1E15)
0
10
20
30
40
50
60
260
262
264
266
268
270
OBSERVATION ANGLE (degrees)

Appendix A

Nomenclature

$f=f(\vec{r},\vec{v},t)$	=	phase space particle density
$\vec{r}$	=	position relative to source
$\vec{v}$	=	velocity of particle in phase space
δ	=	delta function
m	=	mass of molecule
k	=	Boltzmann's constant
T	=	Kelvin temperature
$\vec{\mu}$	=	mean molecule velocity
$n=n(\vec{r},t)$	=	number density
$Q_o(t)$	=	number flux rate from a source
Cos θ	=	$\vec{\mu}\cdot\vec{r}$
t	=	time source is on
$\vec{\nabla}_r$	=	del operator (coordinate)
Φ	=	velocity distribution function
erfc	=	complimentary error function

REFERENCES

1. B. Riley, "Initial Efforts at NASA-Lewis to Model the Self-Induced Molecular Contamination of the Space Station," NASA-ASEE Case-Lewis Summer Faculty Fellowship Program Final Report, 1985 (D123).

2. M.L. BOAS, Mathematical Methods in the Physical Sciences (John Wiley & Sons, New York 1966), pp. 468 & 469.

ACKNOWLEDGEMENTS

The author would like to thank Kent Scheller who programmed the Computer generated figures in this report.

PART 2

0293b

INTRODUCTION

The self-induced molecular contamination around the Space Station could have adverse effects on Space Station components (for example solar panels) as well as scientific experiments (for example experiments involving photons) that might be done on or near the Space Station. One such source of self-induced contaminates is the propulsion system. Consideration is presently being given to continuously or semi-continuously firing small resistojets (in the hundreds of millinewtons thrust range) to overcome on-orbit frictional drag.

This report outlines an initial effort to develop a mathematical model to study the effect of nozzle design on the induced molecular environment around the Space Station produced by simple gas propellants. The mathematical model would allow one to follow the expansion of the gas from the throat of a nozzle to the nozzle exit plane and then into the space external to the nozzle. A description of the proposed two-dimensional model and the mathematical calculations (by numerical methods) that could be performed in a rather complex computer code that must be written to obtain actual predictions are outlined in the remainder of this report.

BASIC APPROACH

Because of the expected relatively low densities of the propellant gas in the region of the exit plane of the nozzle, the fluid flow will be considered from the particle (molecular) nature of the gas using the methods of kinetic-statistical theory. The starting point for describing the gas flow will be the Boltzmann[1] equation for binary collision. In particular, the model described below will be based on the steady state formulation of the BGK approximation(2) or "first iterate equation"(3) of the Boltzmann equation. Then by an iterative process a solution to the Boltzmann equation is obtained.

MATHEMATICAL FORMULATIONS

For the steady state the first iterate equation in differential form is

$$\vec{v} \cdot \vec{\nabla}_r f(\vec{r}, \vec{v}) = A n_e(\vec{r}) \left(f_e - f \right) \tag{1}$$

where Maxwellian molecules[4] have been assumed for describing the interparticle collisions. (See Appendix for equation symbol meanings.) With the appropriate boundary conditions, the first order solution to equation (1) can be obtained. Then the following first moments can be obtained:

$$n(\vec{r}) = \iiint f(\vec{r}, \vec{v}) \, d^3 v \tag{2}$$

$$\vec{u} = \frac{1}{n} \iiint \vec{v} \, f(\vec{r}, \vec{v}) \, d^3 v \tag{3}$$

$$\frac{3}{2} n k T = \frac{m}{2} \iiint (\vec{v} - \vec{u})^2 f(\vec{r}, \vec{v}) \, d^3 v \tag{4}$$

The value of n, $\vec{u}$, T, and f can be the starting values for a second iteration, etc.

Using the method of characteristics equation (1) for can be written in integral form as follows:

$$f(\vec{r}, \vec{v}) = f_B \, e^{-\int_{\vec{S}_0}^{\vec{r}} \frac{A n_e}{v} ds} + \int_{S_0}^{\vec{r}} \frac{A n_e}{v} \left[f_e \, e^{\int_{\vec{S}_0}^{\vec{S}'} \frac{A n_e}{v} ds''} \right] ds' \tag{5}$$

The n_e term is to be determined from one dimensional isentropic flow.

SPECIFIC NOZZLE GEOMETRY AND BOUNDARY CONDITION ASSUMPTIONS

The following section describes the suggested nozzle geometry and boundary conditions for f which can be used to try to simulate the flow of a propellant through a nozzle as well as the flow of the plume. Figure 1 is a diagram of a two-dimensional nozzle and accompanying physical boundaries where $f_B(\vec{r},\vec{v})$ must be specified.

The following boundary conditions (see Figure 1) for f seem appropriate:

$f_{B_1} = 0$ for the inward component of velocity

$$f_{B_{2+}} = \frac{n_B}{(2\pi k T_+/m)^{3/2}} e^{-\frac{m}{2kT_+}(\vec{v}-\hat{i}\,u_x)^2}$$

$$f_{B_{2-}} = 0$$

$$f_{B_3} = 0$$

$$f_{B_4} = \frac{\rho_B}{(2\pi k T_B/m)^{3/2}} e^{-\frac{mv^2}{2kT_B}}$$ diffuse scattering

where n_B and ρ_B are number densities on the respective boundaries. In Figure 1, the outer boundary B_1 is assumed to be approaching infinity thus the number of particles with an inward component of velocity is zero. The number of particles on the outer surfaces $(B_3 + B_{2-})$ of this nozzle is assumed to be zero. The value of f at B_{2+} is assumed to be that obtained from isentropic flow conditions at the throat of the nozzle. In Figure 1 the inside nozzle wall boundary conditions are for complete diffuse scattering, but spectral conditions could also be applied.

DISCUSSION

Within the limitation of this model, one would be able to predict from throat conditions the number density at all points in space. Thus, with the model one can generate number densities at all points around the nozzle as well as number densities near the lip of the nozzle where back flow may be significant.

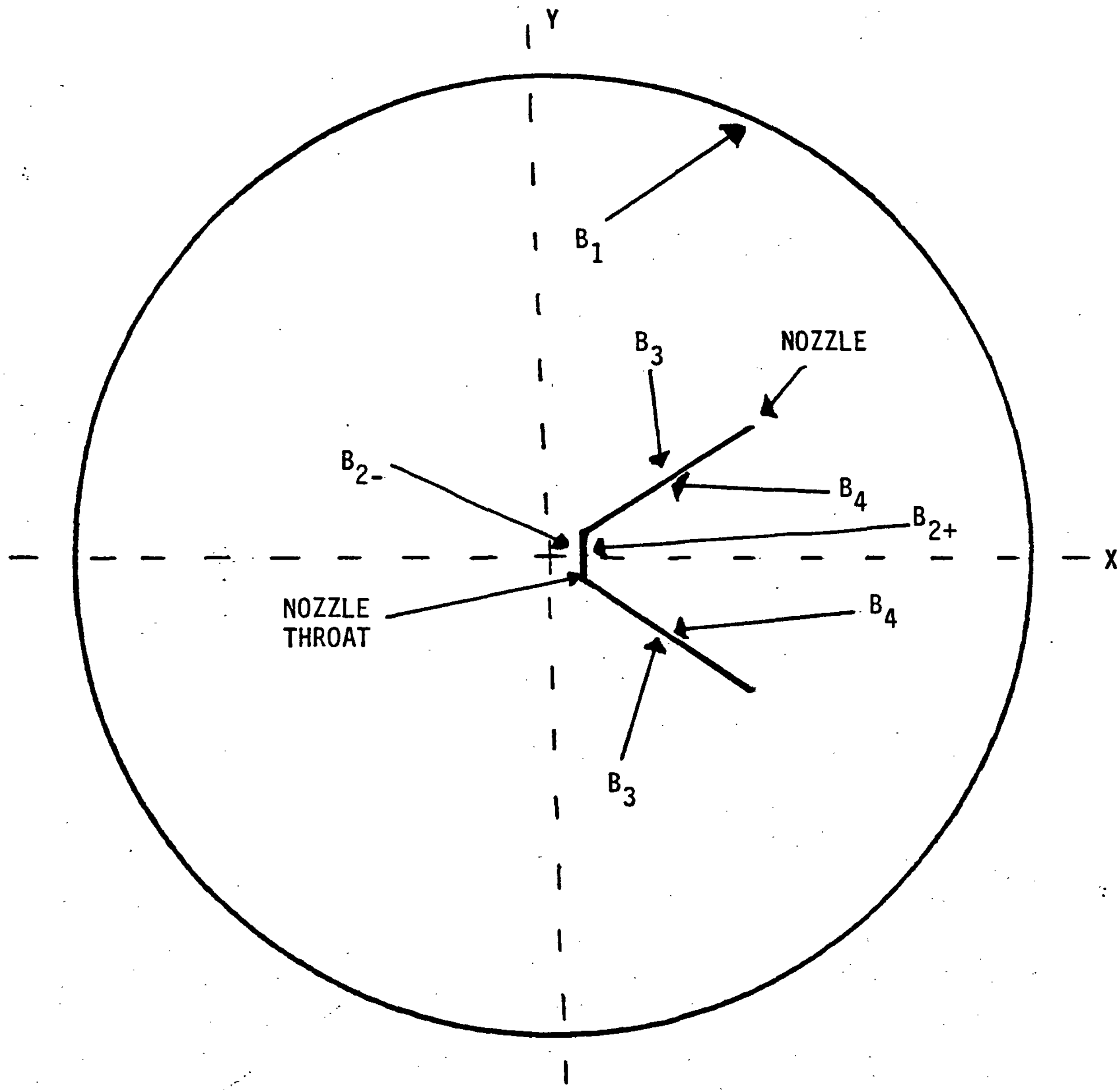

FIGURE 1

APPENDIX

A	= constant
ds	= length in characteristic direction
$f(\vec{r},\vec{v})$	= phase space particle density
f_B	= phase space particle density at boundary
fe	= Maxwellian velocity distribution
k	= Boltzmann's constant
m	= mass of molecule
$n(\vec{r})$	= number density
n_B	= number density at boundary
$\vec{r}$	= space position relative to nozzle
$\vec{S}_o$	= location of boundary
T	= local temperature
T_B	= temperature at boundary
T_{B+}	= temperature of gas at throat
$\vec{u}$	= local mean velocity
u_x	= mean velocity at nozzle throat
$\vec{v}$	= velocity
β_B	= number density at boundary
$\vec{\nabla}_r$	= del operator (coordinate)

1. Patterson, Gordon N., Introduction to the Kinetic Theory of Gas Flows, University of Toronto Press, 1971. pp 29-55.

2. Anderson, Donald G., On the steady Krook kinetic equation: part 1, J. Fluid Mech. 26, 17 (1966).

3. Patterson, Gordon H., Introduction to the Kinetic Theory of Gas Flows, University of Toronto Press, 1971. p 81.

4. Kogan, Mikhail N., Rarefield Gas Dynamics, Plenum Press, New York, 1969. p 41.